AGU PUBLICATIONS

JGR

Journal of Geophysical Research: Biogeosciences

RESEARCH ARTICLE

10.1002/2015JG002988

Key Points:
- N cycle dynamics in LPJ-GUESS improve predictions mainly in boreal forests
- Low absolute effect of N deposition on C sequestration in boreal forests
- N deposition contributes 19% to recent and 24% to historical land C sink

Supporting Information:
- Supporting Information S1

Correspondence to:
K. Fleischer,
k.fleischer@vu.nl

Citation:
Fleischer, K., et al. (2015), Low historical nitrogen deposition effect on carbon sequestration in the boreal zone, *J. Geophys. Res. Biogeosci., 120*, 2542–2561, doi:10.1002/2015JG002988.

Received 10 MAR 2015
Accepted 13 NOV 2015
Accepted article online 18 NOV 2015
Published online 18 DEC 2015

©2015. American Geophysical Union. All Rights Reserved.

Low historical nitrogen deposition effect on carbon sequestration in the boreal zone

K. Fleischer[1], D. Wårlind[2], M. K. van der Molen[3], K. T. Rebel[4], A. Arneth[5], J. W. Erisman[1,6], M. J. Wassen[4], B. Smith[2], C. M. Gough[7], H. A. Margolis[8], A. Cescatti[9], L. Montagnani[10], A. Arain[11], and A. J. Dolman[1]

[1]Hydrology and Geo-Environmental Sciences, Faculty of Life and Earth Sciences, VU University Amsterdam, Amsterdam, Netherlands, [2]Department of Physical Geography and Ecosystem Science, Lund University, Lund, Sweden, [3]Meteorology and Air Quality Group, Wageningen University, Wageningen, Netherlands, [4]Environmental Sciences Group, Copernicus Institute of Sustainable Development, Faculty of Geosciences, Utrecht University, Utrecht, Netherlands, [5]Division of Ecosystem-Atmosphere Interactions, Karlsruhe Institute of Technology, Institute of Meteorology and Climate Research/Atmospheric Environmental Research, Garmisch-Partenkirchen, Germany, [6]Louis Bolk Institute, Driebergen, Netherlands, [7]Department of Biology, Virginia Commonwealth University, Richmond, VA, Canada, [8]Centre for Forest Studies, Faculty of Forestry, Geography, and Geomatics, Laval University, Quebec, Canada, [9]European Commission, Joint Research Centre, Institute for Environment and Sustainability, Ispra, Italy, [10]Faculty of Science and Technology, Free University of Bolzano, Bolzano, Italy, [11]School of Geography and Earth Sciences and McMaster Centre for Climate Change, McMaster University, Hamilton, ON, Canada

Abstract Nitrogen (N) cycle dynamics and N deposition play an important role in determining the terrestrial biosphere's carbon (C) balance. We assess global and biome-specific N deposition effects on C sequestration rates with the dynamic global vegetation model LPJ-GUESS. Modeled CN interactions are evaluated by comparing predictions of the C and CN version of the model with direct observations of C fluxes from 68 forest FLUXNET sites. N limitation on C uptake reduced overestimation of gross primary productivity for boreal evergreen needleleaf forests from 56% to 18%, presenting the greatest improvement among forest types. Relative N deposition effects on C sequestration (dC/dN) in boreal, temperate, and tropical sites ranged from 17 to 26 kg C kg N^{-1} when modeled at site scale and were reduced to 12–22 kg C kg N^{-1} at global scale. We find that 19% of the recent (1990–2007) and 24% of the historical global C sink (1900–2006) was driven by N deposition effects. While boreal forests exhibit highest dC/dN, their N deposition-induced C sink was relatively low and is suspected to stay low in the future as no major changes in N deposition rates are expected in the boreal zone. N deposition induced a greater C sink in temperate and tropical forests, while predicted C fluxes and N-induced C sink response in tropical forests were associated with greatest uncertainties. Future work should be directed at improving the ability of LPJ-GUESS and other process-based ecosystem models to reproduce C cycle dynamics in the tropics, facilitated by more benchmarking data sets. Furthermore, efforts should aim to improve understanding and model representations of N availability (e.g., N fixation and organic N uptake), N limitation, P cycle dynamics, and effects of anthropogenic land use and land cover changes.

1. Introduction

Nitrogen (N) availability plays a central role in driving plant productivity [*Field and Mooney*, 1986; *Kergoat et al.*, 2008; *LeBauer and Treseder*, 2008; *Matear et al.*, 2010; *Fisher et al.*, 2012]. N deposition is strongly affecting carbon (C) cycling and storage due to stoichiometric controls, potentially enhancing productivity and growth, or causing chemical imbalances if exceeding N demands [*Aber et al.*, 1998]. From experimental and monitoring studies, we know that historical increases in atmospheric N deposition in industrialized regions such as North America and Europe significantly contribute to the historical and present terrestrial C sink, particularly enhancing plant growth in N-limited areas [*Sutton et al.*, 2008; *De Vries et al.*, 2009; *Thomas et al.*, 2010; *Fleischer et al.*, 2013]. In concert with rising atmospheric carbon dioxide (CO_2) levels, climate warming, and land use changes [*Churkina et al.*, 2010; *Jain et al.*, 2013], N deposition is a major determinant of ecosystem productivity and functioning [*Galloway et al.*, 2003, 2008; *Gruber and Galloway*, 2008] and the global climate system [*Thornton et al.*, 2009; *Arneth et al.*, 2010; *Erisman et al.*, 2011; *Zaehle et al.*, 2011].

The interaction between forest productivity and N cycle dynamics differs broadly among forest biomes. Strong control of N availability on productivity and growth is believed to play a central role in boreal and temperate forests [*Jarvis and Linder*, 2000; *Fleischer et al.*, 2013; *Smith et al.*, 2014], due to the strong temperature control on N mineralization and general limiting N in soils [*Vitousek and Howarth*, 1991]. Temperate ecosystems

experience lower degrees of N limitation due to historically high rates of N deposition [*Högberg*, 2011], potentially causing N saturation at regional scale [*Aber et al*., 1998; *Brumme and Khanna*, 2008]. Tropical forests are believed to be least affected by N cycle dynamics due to more prevailing phosphorous (P) limitation of old weathered soils in tropical regions [*Vitousek et al*., 2010; *Cleveland et al*., 2011; *Castanho et al*., 2013].

The significance of coupled N and C cycles is increasingly recognized as N dynamics become progressively incorporated into global C cycling models [*Sokolov et al*., 2008; *Jain et al*., 2009; *Churkina et al*., 2010; *Esser et al*., 2011; *Wang et al*., 2010; *Zaehle and Friend*, 2010; *Smith et al*., 2014]. Fertilization experiments and modeling studies point toward an N deposition effect range of 15–40 kg C sequestered per kilogram of N deposited in temperate and boreal forest sites [*De Vries et al*., 2009; *Butterbach-Bahl et al*., 2011; *Erisman et al*., 2011]. Also, in tropical forests, positive growth responses to N availability have been measured [*LeBauer and Treseder*, 2008], although the number of studies is very limited compared to those in temperate and boreal forests. While it is evident that N cycle dynamics have the potential to alter the spatiotemporal distribution and magnitude of the terrestrial C sink [*Le Quéré et al*., 2013], the relative importance of CN interactions, including the precise contribution of N deposition on the past and future C sink, is not yet well constrained at global and regional scales [*Zaehle et al*., 2010; *Wassen et al*., 2013; *Jain et al*., 2013; *Wårlind et al*., 2014].

Discrepancies can partly be ascribed to the fact that CN interactions vary in time and space due to the heterogeneity of underlying factors influencing the fate of C and N in ecosystems, e.g., edaphic characteristic, forest age, nutrient deposition load, microbial and plant N demands, and plant C allocation strategies [*Janssens and Luyssaert*, 2009; *Högberg*, 2011]. These interactions result in large local and regional variations in how N availability relates to forest productivity. Fertilization experiments are furthermore not directly translatable to real-world scenarios, while observational studies are inevitably hampered by the challenge to separate effects of N deposition from other confounding factors [*Fleischer et al*., 2013; *Sutton et al*., 2008]. Not least in importance, we lack essential knowledge on the magnitude of acting drivers of key processes in the N cycle, such as N fixation or denitrification, which are generally too simplistically represented in process-based ecosystem models [*Zaehle and Dalmonech*, 2011; *Wårlind et al*., 2014].

One such ecosystem model, the global dynamic vegetation model (DGVM) LPJ-GUESS [*Smith et al*., 2001; *Sitch et al*., 2003; *Smith et al*., 2014], has been widely applied at regional and global scales to address questions of ecosystem function in response to environmental changes [*Morales et al*., 2005; *Jung et al*., 2007; *Smith et al*., 2008; *Hickler et al*., 2008, 2012; *Ahlström et al*., 2012; *Wårlind et al*., 2014]. An original feature of LPJ-GUESS is that it includes vegetation dynamics and stochasticity, allowing biome shifts and disturbance regimes to be simulated. Various aspects of C and N cycle dynamics in LPJ-GUESS have been evaluated by *Smith et al*. [2014], such as site-scale net primary productivity (NPP) and the sensitivity of the C cycle to warming and CO_2 fertilization. Highlighting the regional differences in CN interactions, *Smith et al*. [2014] found that N cycle dynamics had little effect on C fluxes globally, but regional patterns have been altered. Temperature and moisture controls on soil organic matter dynamics and N mineralization have reduced productivity in boreal, arctic, and water-limited ecosystems in the midlatitudes. Well-watered temperate ecosystems and the tropics on the other hand were not affected [*Smith et al*., 2014]. *Wårlind et al*. [2014] have given a first estimate of N deposition effect on the terrestrial C balance using LPJ-GUESS, which induced 55 Pg C to be sequestered from 1850 to 2100.

Our objective is to contribute to the understanding of regional variations of CN interactions and their impacts on C dynamics by (1) extending the evaluation of N cycle dynamics in LPJ-GUESS, using direct FLUXNET observations of C fluxes at the site scale and other independent observations of C pools and key N cycle variables, to assess how N cycle dynamics affect prediction accuracy in different forest types and climate zones, and (2) by quantifying the effect of N deposition on historical C sequestration for different forest types and climate zones, contrasting results from site and global simulations.

We evaluate the simulated daily and annual C fluxes from the C and CN version of LPJ-GUESS with direct observations of C fluxes from 68 FLUXNET forest sites encompassing the world's major forest types. We further evaluate predictions of biomass and soil C pools, as well as foliar N and leaf area index (LAI) as key dynamic variables affecting the C cycle. Due to the regional differences in CN interactions in forest ecosystems, we expect impacts of N dynamics on C flux simulations to differ between sites and forest types. The CN model version is then employed to assess the effect of N deposition on C sequestration, in relative and absolute terms, from site and global simulations. In doing so, we contrast effects between forest types and climate

zones in order to assess regional variations of CN interactions. As detailed above, we expect to see the greatest improvements due to the N cycle inclusion in boreal forests, and consequently the greatest C sequestration response to N deposition. We expect less effects of N cycle dynamics and N deposition in temperate forests and little to no effect in tropical forests.

Site-scale simulations assess the N deposition effect for a particular stand of forest over its lifetime, excluding major disturbances and vegetation composition changes in site simulations. Global simulations, on the other hand, include nonforest ecosystems, disturbances, and changes in vegetation distribution; thus, N deposition effects are expected to be dampened. The combined examination of N deposition effects at site and global scales, to our knowledge, is unique and has the potential to identify differences arising when assessing N deposition at global scale versus upscaling site-scale effects.

2. Methods

2.1. LPJ-GUESS and the N Cycle

LPJ-GUESS is a process-based global dynamic vegetation model [*Smith et al*., 2001; *Sitch et al*., 2003] that has recently been extended to include key N cycling processes and feedbacks between the vegetation and soil C and N cycles [*Smith et al*., 2014]. LPJ-GUESS predicts vegetation structure and dynamics based on weather, atmospheric CO_2 concentration, N deposition, and soil texture. The model includes 12 plant functional types (PFTs) with varying bioclimatic limits and life traits, determining establishment and competition. Age cohorts of the different PFTs allow realistic population structures to develop, which is a unique feature of LPJ-GUESS in contrast to other models applied at global scale [*Zaehle et al*., 2014]. A detailed description of the physiological processes and representations of the carbon, water, and energy cycle in LPJ-GUESS are summarized elsewhere [*Smith et al*., 2001; *Sitch et al*., 2003; *Hickler et al*., 2012].

LPJ-GUESS dynamically simulates the N cycle, including plant uptake, allocation, turnover, fixation, mineralization, denitrification, and leaching of N, for which underlying processes have been explained and emerging N fluxes and stocks have been evaluated in detail by *Smith et al*. [2014]. N input originates from biological N fixation, empirically simulated as a function of annual evapotranspiration [*Cleveland et al*., 1999] and N deposition [*Lamarque et al*., 2010], given as dry and wet depositions. N is lost from the ecosystems via leaching and a simplified representation of denitrification [*Thomas et al*., 2013]. Interactions between the C and N cycles in LPJ-GUESS include (1) dependency of photosynthesis and plant respiration on leaf/plant tissue N, (2) limitation of decomposition by N availability, (3) dependency of shoot and root C allocation on the C:N ratio of these tissues, and (4) limitation of N uptake by fine root mass. The calculation of foliar N concentrations and C:N ratios of plant tissues and soil compartments allows N to impose constraints on productivity, respiration, and C allocation.

2.2. FLUXNET Data

FLUXNET is a global network of sites where the ecosystem carbon, water, and energy exchanges are continuously monitored by the eddy covariance methodology [*Baldocchi et al*., 2001]. FLUXNET data have become a benchmark for ecosystem models due to their high temporal resolution and relatively broad regional coverage [*Medlyn et al*., 2005b; *Friend et al*., 2007; *Williams et al*., 2009]. Observations from 68 forest FLUXNET sites (La Thuile data set, Table A1) [*Baldocchi et al*., 2001] from 1995 to 2008 were compiled, resulting in 226 site years with 1 to 9 site years per site. The sites represent a diverse range of forest types and climate zones between 68.4°N and 10.1°S with N deposition rates from 1.5 to 21.8 kg N ha^{-1} yr^{-1} [*Lamarque et al*., 2010]. The dominant forest types in the data set are boreal evergreen needleleaf forests (BNE) ($n = 28$), temperate deciduous broadleaf forests (TeBS) ($n = 15$), and temperate evergreen needleleaf forests (TeNE) ($n = 13$), mainly situated in Europe, the Northern U.S. and Canada (Table A1). FLUXNET sites measure half-hourly biosphere-atmosphere C fluxes at the ecosystem scale, simultaneously with meteorological conditions. Daily site meteorology was used as input to LPJ-GUESS. We disregarded site years with incomplete annual meteorological data ($n < 365$), as well as years with more than 20% of daily fluxes missing or flagged as low quality (<0.90) in the FLUXNET La Thuile data set.

FLUXNET sites were originally classified according to PFT and climate, based on recommendations by the International Geosphere-Biosphere Program (IGBP) [*Loveland et al*., 2000] and the Köppen-Geiger climate classification [*Kottek et al*., 2006]. The sites were reclassified according to the PFT classification system within LPJ-GUESS [*Sitch et al*., 2003; *Ahlström et al*., 2012], covering the following PFTs: BNE = boreal needleleaf evergreen, TeNE = temperate needleleaf evergreen, TeBS = shade-tolerant temperate broadleaf summergreen,

Table 1. Overview of Local and Global Simulations Run of LPJ-GUESS, Including Model Version Carbon-Only (C) or Carbon-Nitrogen (CN), Run Code, N Deposition Scenario ("Actual" for Rising N Deposition and "Preindustrial" for Stagnant N Deposition Form the Year 1850), Time Period of Simulations, and Source of Meteorological Input

Version	Run	N Deposition	Simulation Period	Meteorology
			Site-Scale Model Simulations	
C	C-Ac-L	--	forest lifetime (since last major disturbance to 2006)	CRU climate[a], corrected with tower-based meteorology
CN	CN-Ac-L	Actual		
CN	CN-Pi-L	Preindustrial		
			Global-Scale Model Simulations	
CN	CN-Ac-G	Actual	1901–2006	CRU climate[a]
CN	CN-Pi-G	Preindustrial	1901–2006	

[a]CRU (Climate Research Unit) climate data [*Mitchell and Jones*, 2005].

TrBE = tropical evergreen broadleaf. Mixed forests (MF) in FLUXNET do not correspond to a particular PFT in LPJ-GUESS and were classified as potential natural vegetation which included all woody PFTs.

2.3. Modeling Protocol

The effects of N cycle dynamics on model performance were tested by running site-scale simulations of the 68 FLUXNET sites using the C and CN version of the model (Table 1). The evaluation setup extends previous work by *Morales et al*. [2005] who tested predictions by LPJ-GUESS and other models of C and water fluxes at 15 European FLUXNET sites. For both model versions, identical modeling protocols for the spin-up and simulation phase, as well as identical climatic drivers and CO_2 concentrations, were employed. To be able to assess the effects of N dynamics only, all parameters shared between the C and CN version were set equal. In particular, the quantum efficiency scalar α_a was set to the same value (0.7) for all PFTs for both the C and CN version of the model, with further explanation in Text Box A1. The CN version of the model was then employed at site and global scales to assess the effect of N deposition on C sequestration (Table 1). In both cases, this was done by contrasting C sequestration rates of the original run using actual historical N deposition (CN-Ac-L/G) with an additional run where N deposition remained at preindustrial levels (CN-Pi-L/G).

The 500 year long spin-up period, with preindustrial climate, CO_2 and N deposition, ends in 1901 with C and N stocks in equilibrium. This spin-up routine was employed for both local and global simulations. The following input was continuously repeated during the spin-up: monthly CRU TS 3.0 climate data from 1901 to 1930 (Climate Research Unit) [*Mitchell and Jones*, 2005], preindustrial levels of atmospheric CO_2 from 1901 [*McGuire et al*., 2001], and for the CN version modeled N deposition estimates from the year 1850 [*Lamarque et al*., 2010]. The simulation phase commences in 1901 with atmospheric CO_2 concentration and CRU climate representing the historical industrial period [see also *Morales et al*., 2005; *Thornton et al*., 2007; *Churkina et al*., 2010], and the N deposition scenario commences in 1850. This routine follows current best practices in terrestrial vegetation models [*Williams et al*., 2009].

Site simulations were optimized by passing local information to the model, namely, tower-based meteorology, stand age, and dominant PFT. For sites with discontinuous site years included in the analysis, the nearest $0.5 \times 0.5°$ grid cell of the CRU climate data was detrended and bias corrected against tower-based meteorology. The time of the last major stand-replacing disturbance was extracted from FLUXNET and the literature to derive stand age (see Table A1) [*Fleischer et al*., 2013]. At that time, a clearance of the forest was simulated, removing all aboveground biomass, after which only the PFT present at the FLUXNET sites was allowed to establish. Sites were excluded from the analysis when the prescribed PFT did not establish due to prescribed bioclimatic limits in LPJ-GUESS. Global simulations were run from 1901 to 2006 at a $0.5 \times 0.5°$ resolution initialized after the spin-up routine. Atmospheric CO_2 [*McGuire et al*., 2001], CRU climate data [*Mitchell and Jones*, 2005], and N deposition [*Lamarque et al*., 2010] are passed as inputs throughout the historical period.

Physiological processes and associated C, N, and water fluxes are simulated on a daily time step and were run over 20 replicate patches at site scale and 5 replicate patches at global scale. Multiple patches represent stochastic variation in growth processes and disturbance events, and modeled values are averages of the resulting vegetation dynamics [see *Smith et al*., 2001]. Stochastic disturbances, representing total loss of vegetation in a patch, due to e.g. storms or fire, were implemented for a mean interval of 100 years for site and global simulations (at site scale not after prescribed stand establishment).

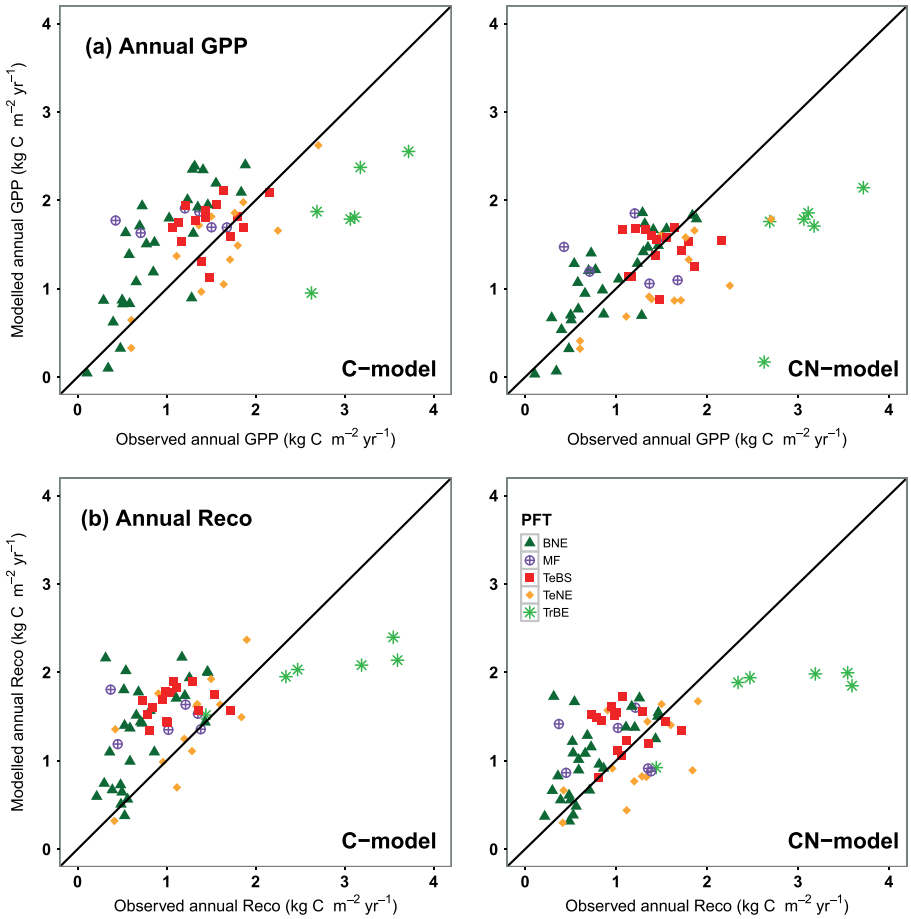

Figure 1. Observed versus modeled annual gross primary production (GPP) and ecosystem respiration (R_{eco}), averaged per forest site ($n = 68$), in kg C m^{-2} yr^{-1} for both (left) the C version and (right) the CN version of LPJ-GUESS; symbols reflect the PFT classification of LPJ-GUESS; see legend.

2.4. Model Evaluation

We evaluated site simulations per PFT against observations for the following annual C fluxes: gross primary productivity (GPP), representing total ecosystem carbon uptake by photosynthesis; ecosystem respiration (R_{eco}), representing the sum of autotrophic (R_a) and heterotrophic (R_h) respiration; and net ecosystem C exchange (NEE). NEE is reported following the Intergovernmental Panel on Climate Change convention, with negative values representing an uptake of C by the ecosystem and positive values a loss of C to the atmosphere, i.e., $-\mathrm{NEE} = \mathrm{GPP} - R_{eco}$. We then evaluated the seasonality of daily GPP and R_{eco} against observed fluxes per PFT, for which multiple years per site were averaged first. Predictions of foliar N and LAI were compared to a set of ancillary observations taken at FLUXNET sites [*Fleischer et al.*, 2013], representing their seasonal maximum. As consistent information on C pool sizes is not available within FLUXNET, we evaluated predicted biomass and soil C pools using two independent data sets each. For biomass, we use spatially explicit estimates from *Ruesch and Gibbs* [2008] and estimates for major global biomes in *Luysseart et al.* [2007]. For soil C, we use spatially explicit estimates from the Harmonized World Soil Database (HWSD) [*FAO/IIASA/ISRIC/ISSCAS/JRC*, 2012] and biome averages from *Zinke et al.* [1984]. Model data agreement was assessed by their root mean square error (RMSE), and the tendency of the model to overestimate or underestimate was measured by percent bias (Pbias) [*Maréchal*, 2004].

2.5. N Deposition Effect

The historical N deposition effect was assessed for different forest types and climate zones in terms of its relative effect (i.e., C sequestration per unit N deposition, hereafter dC/dN) and its absolute effect on C sequestration (i.e., the amount of C sequestered due to N deposition). The relative N deposition effect was derived in an

Table 2. Mean and Standard Deviations of Major C Fluxes (GPP, R_{eco}, and NEE) From Observations and Models and Error Metrics for C and CN Version (RMSE and Pbias) as Evaluated Against Observations, Computed for All Sites (ALL) and Per PFT[a]

		Observation		C model		CN model		RMSE		Pbias	
		Mean	SD	Mean	SD	Mean	SD	C	CN	C	CN
GPP	ALL	1.38	0.75	1.58	0.58	1.24	0.49	0.65	0.63	14.2	−10.5
	MF	1.15	0.48	1.76	0.11	1.38	0.31	0.76	0.60	53.4	19.9
	TrBE	3.07	0.39	1.89	0.56	1.57	0.70	1.21	1.57	−38.3	−48.7
	TeNE	1.56	0.59	1.45	0.60	1.07	0.48	0.34	0.60	−7.3	−31.3
	BNE	0.92	0.48	1.44	0.70	1.09	0.52	0.66	0.34	56.2	18.3
	TeBS	1.49	0.30	1.74	0.27	1.45	0.25	0.41	0.37	16.3	−3.0
R_{eco}	ALL	1.10	0.70	1.49	0.49	1.18	0.45	0.69	0.56	35.3	7.3
	MF	0.97	0.45	1.48	0.22	1.18	0.33	0.70	0.57	53.1	21.6
	TrBE	2.76	0.84	2.02	0.29	1.76	0.42	0.92	1.13	−27.0	−36.2
	TeNE	1.22	0.46	1.40	0.54	1.03	0.47	0.44	0.45	14.7	−15.6
	BNE	0.73	0.37	1.34	0.56	1.03	0.44	0.76	0.47	83.1	40.8
	TeBS	1.09	0.28	1.65	0.17	1.37	0.25	0.63	0.46	52.3	26.7
NEE	ALL	−0.28	0.36	−0.09	0.23	−0.05	0.16	0.48	0.47	−69.3	−81.1
	MF	−0.18	0.19	−0.28	0.16	−0.20	0.09	0.20	0.17	55.1	10.6
	TrBE	−0.30	0.57	0.13	0.30	0.19	0.30	0.86	0.87	−142.7	−163.7
	TeNE	−0.35	0.33	−0.05	0.12	−0.05	0.08	0.43	0.44	−85.1	−86.6
	BNE	−0.19	0.39	−0.10	0.20	−0.06	0.13	0.41	0.42	−45.9	−67.2
	TeBS	−0.41	0.24	−0.09	0.27	−0.08	0.14	0.52	0.46	−79.1	−81.5

[a]Mixed forests (MF), tropical evergreen broadleaf forests (TrBE), temperate evergreen needleleaf forests (TeNE), boreal evergreen needleleaf forests (BNE), and temperate broadleaf summergreen forests (TeBS). Mean, SD, and RMSE of C fluxes expressed in kg C m^{-2} yr^{-1} and Pbias expressed in percent bias.

identical fashion for site and global simulations. For that, we compared differences in C pools (ΔC pool) from two contrasting simulations, one with rising N deposition (CN-Ac for "actual") and one with preindustrial levels of N deposition (CN-Pi for "preindustrial") (Table 1). We infer the N deposition effect with these runs, as all other potential drivers such as CO_2 concentration, climate, and age of forests were identical. We calculated dC/dN as ΔC pool/ΔN deposition, where ΔN deposition is the difference in cumulative N deposition. For site simulations, we only assessed biomass C pools because soil C pools were perturbed by the prescribed disturbance and often did not recover during the simulation period. For global simulations, we assessed N deposition effects on changes in soil, litter, biomass, and total ecosystem C pools. To further elucidate differences between local- and global-scale simulations, we analyzed signs of N saturation, vegetation distribution shifts, and different N sensitivities in litter, vegetation, and soil C pools in the global simulations.

To complement the global estimate, we additionally employed an upscaling approach to derive the absolute global N deposition effect on forest C sequestration from site estimates. For this, we combined mean N sensitivity of C sequestration rates (dC/dN) per forest type from the site-scale simulations with independent estimates of global forest C budgets [*Pan et al.*, 2011] and mean N deposition rates per forest type. The latter were derived by overlaying PFT distributions from historical land cover change reconstructions for 1990 [*Lawrence et al.*, 2012] with global N deposition for 1990–1999 [*Lamarque et al.*, 2010]. We propagated the uncertainty in dC/dN, C sinks, and N deposition to the potential impact of N deposition on C sink strengths, for which we assumed 50% uncertainty in N deposition estimates [*Dentener et al.*, 2006] and used the 68% confidence interval (CI) of dC/dN to estimate the unknown error.

3. Results

Inclusion of the N cycle in LPJ-GUESS caused an overall reduction in mean annual GPP and R_{eco} estimates of −0.34 kg C m^{-2} yr^{-1} and −0.31 kg C m^{-2} yr^{-1}, respectively (Δ = C − CN). N cycle dynamics caused overall model performance improvement, reducing overall bias of 14% in the C version to −11% in the CN version, while RMSE improved slightly from 0.65 to 0.63 kg C m^{-2} yr^{-1} (Figure 1 and Table 2). N cycle effects differed between forest types as expected (Figure 1 and Table 2). Predictions of GPP improved most strongly for boreal needleleaf forests (BNE), where the CN version reduced overestimation from 56% to 18% with a considerable reduction in RMSE (0.66 to 0.34 kg C m^{-2} yr^{-1}). For temperate deciduous (TeBS), prediction bias of mean GPP improved with the CN version from 16% overestimation to 3% underestimation, while RMSE was slightly reduced. For mixed forests (MF), both error and bias scores improved with the N cycle inclusion (Table 2). For temperate needleleaf (TeNE)

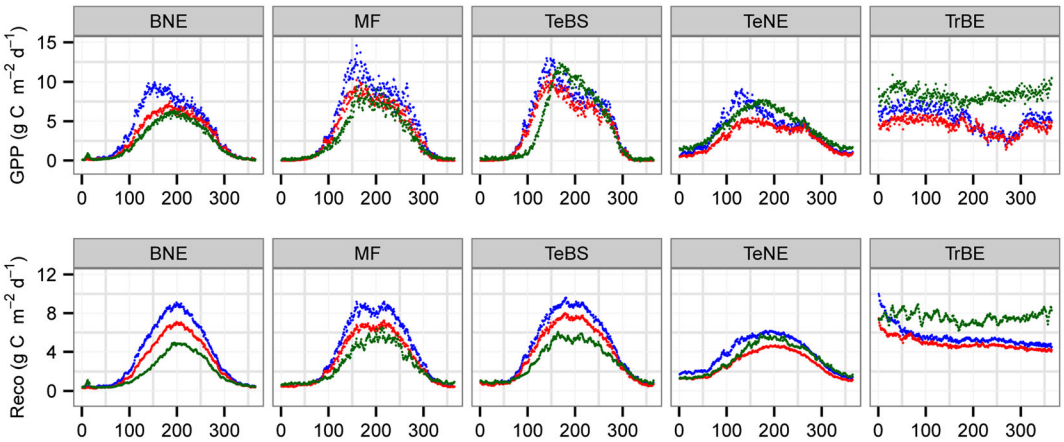

Figure 2. Average seasonal cycle of daily gross primary production (GPP) and ecosystem respiration (R_{eco}) in g C m^{-2} d^{-1} against day of the year for the C version (blue), the CN version (red) of LPJ-GUESS, and FLUXNET observations (green), PFTs in panels from left to right (with number of sites): boreal evergreen needleleaf forests (BNE, $n = 28$), mixed forests (MF, $n = 6$), temperate broadleaf summergreen forests (TeBS, $n = 15$), temperate evergreen needleleaf forests (TeNE, $n = 13$), and tropical evergreen broadleaf forests (TrBE, $n = 6$).

and tropical forests (TrBE), modeled results were comparable, although the C version achieved marginally better accuracy scores. For TrBE, both model versions underestimated mean GPP and had high error and bias scores. Also, annual totals of R_{eco} are predicted with greater accuracy by the CN version, reducing bias from 35% to 7% and RMSE from 0.69 to 0.56 kg C m^{-2} yr^{-1} (Figure 1 and Table 2). The largest improvement occurred for BNE, reducing RMSE from 0.76 to 0.47 kg C m^{-2} yr^{-1} and bias from 83% to 41% (Figure 1 and Table 2). For TeBS and MF, R_{eco} predictions were similarly reduced for both RMSE and bias. For TeNE, RMSE and bias of R_{eco} predictions were comparable in both model versions. TrBE respiration rates were underestimated by both models.

The CN version achieved also the closest agreement between modeled and observed seasonality of C fluxes for BNE (Figure 2). The C version simulates a fast increase of GPP and R_{eco} at the start of the year and an overestimated summer peak, which was diminished with the consideration of N limitations in the CN version. For MF and TeBS, the seasonality in GPP was generally reproduced well by both model versions (Figure 2). For both forest types, the unrealistically high simulated GPP summer maximum was reduced in the CN version, which caused a better match to observations for mixed forests but slightly underestimated the summer peak for TeBS. Peak rates of R_{eco} for MF, TeBS, and BNE were reduced, which improved model fit although an overestimation in summer respiration remained. Seasonality of C fluxes in TrBE was not reproduced well. Magnitudes of GPP and R_{eco} are underestimated, as noted earlier, and both models predicted a strong decline in GPP around day 180, not supported by observations, although CN dynamics reduced the overpronounced seasonal variation to some extent. The unusually high R_{eco} rates for TrBE at the start of the year (Figure 2) are due to the fact that modeled annual litter input occurs on day 1.

FLUXNET observations of NEE show that all forest types included in the analysis are on average C sinks; however, within forest types, the net C uptake was highly variable in sign and magnitude. TeNE and TeBS exhibited the largest mean net C exchange with -0.35 ± 0.33 and -0.41 ± 0.24 kg C m^{-2} yr^{-1}, respectively (Table 2). TrBE showed a lower mean net C exchange of -0.30 ± 0.57 kg C m^{-2} yr^{-1}, and BNE and MF exhibited the weakest net C exchange with -0.19 ± 0.39 and -0.18 ± 0.19 kg C m^{-2} yr^{-1}, respectively. Both models generally underestimated the observed mean NEE and achieved similar accuracy scores in predicting NEE across and within PFTs (Table 2). This was also the case for BNE, despite the better accuracy scores for GPP and R_{eco} in the CN version, as overestimations in both GPP and R_{eco} canceled each other out in the C version. For TrBE, both models predicted a C source in contrast to the observed substantial C sink. Only for MF did the CN version achieve satisfactory NEE predictions, reducing RMSE to 0.17 kg C m^{-2} yr^{-1} and bias to 11%.

Mean C pools in biomass and soil were consistently reduced in the CN version compared to the C version across all forest types (Figure 3). This reduction generally resulted in better agreement with observations, with some exceptions. There is considerable variation and hence uncertainty in soil and biomass C estimates,

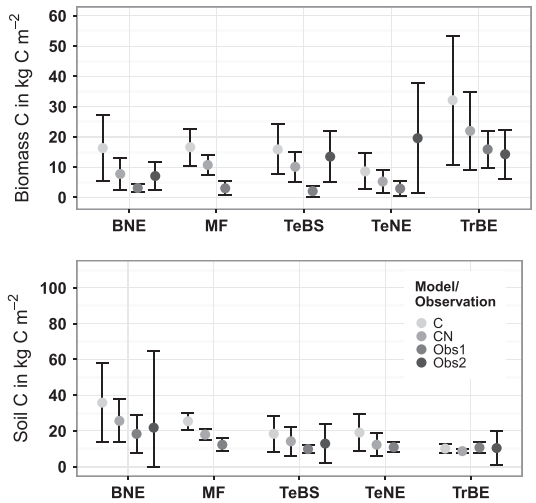

Figure 3. Mean biomass and soil C pools in kg C m^{-2} for C and CN version averaged per PFT compared to observations by *Ruesch and Gibbs* [2008] (Obs1) and *Luysseart et al.* [2007] (Obs2) for biomass C and the HWSD [*FAO/IIASA/ISRIC/ISSCAS/JRC*, 2012] (Obs1) and *Zinke et al.* [1984] (Obs2) for soil C; error bars represent 1 standard deviation. PFTs with number of modeled sites are boreal evergreen needleleaf forests (BNE, $n = 28$), mixed forests (MF, $n = 6$), temperate broadleaf summergreen forests (TeBS, $n = 15$), temperate evergreen needleleaf forests (TeNE, $n = 13$), and tropical evergreen broadleaf forests (TrBE, $n = 6$).

complicating a clear comparison; e.g., biomass C estimates from *Ruesch and Gibbs* [2008] are very low compared to estimates from *Luysseart et al.* [2007]. However, for forest types in which observational estimates of biomass are in closer agreement with each other, like BNE (3 and 7 kg C m^{-2}) and TrBE (16 and 14 kg C m^{-2}), the CN version is closer to observations, with ~8 and 22 kg C m^{-2}, respectively. The CN version is also closer to the one available MF observation of 3 kg C m^{-2} with 11 kg C m^{-2}. For the other forest types, TeBS and TeNE, the comparison remains inconclusive. Soil C observations are in better agreement with each other than biomass C observations. BNE observations of ~18 and 22 kg C m^{-2} are best simulated in the CN version with ~26 kg C m^{-2} (Figure 3). For TrBE, both model versions were in very good agreement with observations of soil C between 9 and 11 kg C m^{-2}. For TeBS, mean soil C at 14 kg C m^{-2} in the CN version is closest to both available observations at 10 and 13 kg C m^{-2}. For MF and TeNE, only one soil C observation was available, which was in better agreement with estimates of the CN version (Figure 3).

Maximum foliar N concentrations in the CN version of LPJ-GUESS agreed well with observations (Figure 4). N cycle dynamics and flexible stoichiometry in the CN version induced realistically greater variation in foliar N compared to the C version, which simulated very constrained foliar N values due to fixed C:N ratios (not shown). Consequently, performance was markedly improved by the CN version, reducing RMSE from 0.58% to 0.38% N and bias from −29% to −4%. Notably, the agreement is largely driven by simulations capturing the differences between needleleaf (BNE) and broadleaf species (TeBS). Within PFT, agreement is limited, as the CN version does not capture the full range of observed variations in foliar N within PFTs (Figure 4). The agreement of simulated maximum LAI with field measurements was poor, in that both model

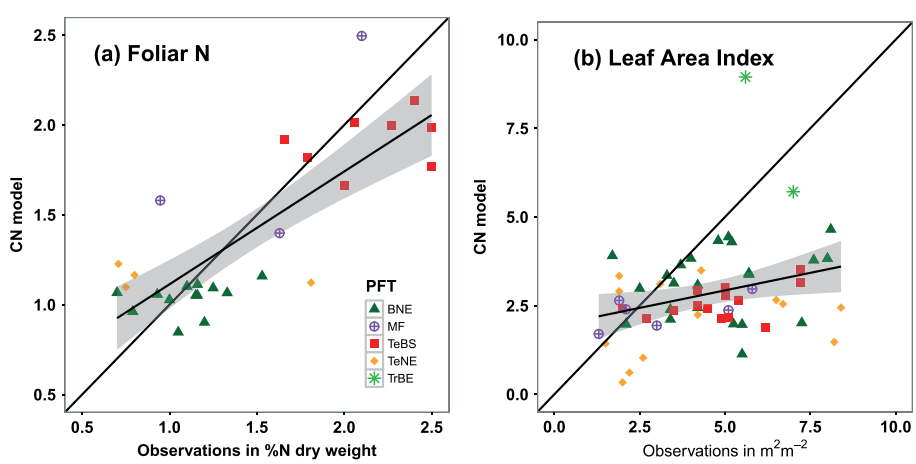

Figure 4. Scatterplot of observed versus simulated values averaged per site for the CN version for (a) maximum foliar N in %N per dry weight ($n = 28$) and (b) maximum leaf area index (LAI) in m^2 m^{-2} ($n = 59$). Color and shape represent PFT classification in LPJ-GUESS (see legend). The 1:1 line in black and the linear regression line with 1 SE underlain in grey.

Table 3. C Sequestration Per Unit N Deposition (dC/dN), Age, and N Deposition Loads Per PFT and Climate Zone From Site-Scale Simulations ($n = 68$)[a]

		dC/dN						Total N deposition	
	n	mean	SD	min	max	CI[b]	Age years	(Δ) kg N ha^{-1}	(CN-Ac-G) kg N ha^{-1}
					PFT				
BNE	28	19.6	13.7	−18.3	41.2	2.6	83.4	247.7	373.7
MF	6	27.7	30.5	−13.0	74.9	13.8	101.0	405.5	559.5
TeBS	15	21.6	16.1	−2.6	48.4	4.3	74.2	436.1	672.1
TeNE	13	25.6	17.2	0.1	49.7	4.9	53.4	235.8	298.0
TrBE	6	25.9	23.9	−6.8	58.5	10.8	147.7	106.5	285.2
					Climate				
Boreal	14	17.5	18.7	−18.3	41.2	5.2	77.1	152.9	226.7
Temperate	47	24.0	16.1	−2.6	74.9	2.4	77.1	355.9	521.0
Tropical	6	25.9	23.9	−6.8	58.5	10.8	147.7	106.5	285.2

[a]Mean, 1 standard deviation (SD), minimum (min), maximum (max), and 68% confidence interval (CI) given for dC/dN in kg C kg N^{-1}, mean age in years, mean difference in total N deposition between actual and preindustrial runs Δ (CN-Ac-G, CN-Pi-G), and mean total load in actual run (CN-Ac-G). Data summarized per PFT (boreal evergreen needleleaf forests (BNE), mixed forests (MF), temperate broadleaf summergreen forests (TeBS), temperate evergreen needleleaf forests (TeNE), and tropical evergreen broadleaf forests (TrBE)) and climate zone (boreal, temperate, and tropical).
[b]Given as 68% confidence interval, assuming Gaussian error distributions that the real value lies within the given interval.

versions did not reproduce the slope or the range of observed values (Figure 4). Observed LAI ranged from ~1 to 8 m^2 m^{-2}, whereas simulations did not exceed 5 m^2 m^{-2} for both model versions. N cycle inclusion reduced mean LAI relative to the C version (not shown) from 3.3 to 2.8 m^2 m^{-2}, compared to an observed 4.4 m^2 m^{-2}. The N cycle thus slightly reduced the performance in simulating maximum LAI in terms of RMSE (from 2.4 to 2.5 m^2 m^{-2}) and bias (from −26% to −37%).

C sequestration per unit N deposition from site-scale simulations ranged from −18 to 75 kg C kg N^{-1}, with forest type means from 20 to 28 kg C kg N^{-1} (Table 3). Temperate needleleaf forests (TeNE), mixed forests (MF), and tropical forests (TrBE) experienced highest N sensitivities with 26–28 kg C kg N^{-1}, compared to 20–22 kg C kg N^{-1} for boreal needleleaf forests (BNE) and temperate deciduous broadleaf forests (TeBS) (Table 3). Aggregating sites per climate zone results in a poleward decreasing trend of dC/dN, from 26 kg C kg N^{-1} in tropical sites to 24 kg C kg N^{-1} in temperate and 17.5 kg C kg N^{-1} in boreal sites (Table 3). Temperate forest sites saw by far the highest N deposition loads and rise therein throughout the historical period. Tropical sites experience lower levels of N deposition loads, comparable to boreal sites, but tropical forests were almost twice as old as boreal and temperate forests (Table 3). Large variability of dC/dN occurred within forest types, potentially due to low site data availability, e.g., for tropical sites, but also due to strong site conditional responses to N addition, as standard deviations remained high in temperate sites, for which relatively many sites were available.

Although the representativeness of our site selection to the wider biomes is questionable, biomass dC/dN per biome and PFT are within range of published estimates of 15–40 kg C kg N^{-1} for temperate and boreal forests [*De Vries et al.*, 2009]. Therefore, we employ these estimates to derive the potential global contribution of N deposition to the terrestrial C sink (Table 4). Biomass dC/dN from site simulations amounted to 23 kg C kg N^{-1}

Table 4. Contribution of N Deposition to the Global and Biome-Specific Forest C Sink, Based on Forest Area Per Climate Zone in Megahectare and C Sinks in Pg C yr^{-1} for 1990–2007 From *Pan et al.* [2011], Average N Deposition Per Forest Type in the 2000s kg N ha^{-1} yr^{-1} Based on *Lawrence et al.* [2012] and *Lamarque et al.* [2010] and dC/dN in kg C kg N^{-1} From This Study[a]

	Area	C Sink	dC/dN	N Deposition	N Deposition Effect	
Forest	Mha	P C yr^{-1}	kg C kg N^{-1}	kg N ha^{-1} yr^{-1}	Pg C yr^{-1}	%
Boreal	1135	0.50 ± 0.08	17.5 ± 5.2	3.6 ± 1.8	0.07 ± 0.04	14.3 ± 4.3
Temperate	767	0.72 ± 0.08	24.0 ± 2.4	6.2 ± 3.1	0.11 ± 0.06	15.9 ± 6.0
Tropical[b]	1949	1.19 ± 0.41	25.9 ± 10.8	5.3 ± 2.7	0.27 ± 0.17	22.5 ± 19.7
Global[c]	3851	2.40 ± 0.42	23.0 ± 7.5	5.2 ± 2.6	0.46 ± 0.28	19.2 ± 28.7

[a]The resulting C sink due to N deposition (N deposition effect) is given in Pg C yr^{-1} and in percent of the total C sink. The following uncertainties are propagated to derive the N deposition effect: uncertainty as 68% CI for C sinks (as described in *Pan et al.* [2011]) and for dC/dN (as in Table 3), and uncertainty of N deposition is assumed at 50% [see *Dentener et al.*, 2006].
[b]Including intact tropical forests only (as in *Pan et al.* [2011]).
[c]Global dC/dN calculated as area-weighted mean of climate zone-based dC/dN.

Table 5. Historical C Sequestration Rates and N Deposition Effects for 1900–2006 From Global Simulations, Including Total Area (Mha), Total C Sequestration (Pg C), the Induced C Sequestration due to N Deposition (Pg C) (ΔCN-Ac-G and CN-Pi-G), Total Additional N Deposition (kg N ha^{-1}) (ΔCN-Ac-G and CN-Pi-G), Resulting dC/dN (kg C kg N^{-1}), and the Contribution of N Deposition on Total C Sequestration in Percent (N-Induced C Sink/C Sink)[a]

	Area	C Sink	N-Induced C Sink	Additional N Deposition	dC/dN	N Deposition Effect
	Mha	Pg C	Pg C	kg N ha^{-1}	kg C kg N^{-1}	%
Temperate (N)	3189	31.4	10.7	273.0	12.3	34.0
Boreal	1505	17.7	3.3	100.2	21.7	18.5
Tropical	5042	54.1	11.9	132.5	17.8	22.0
Subtropical	2712	9.2	2.2	140.5	5.6	23.4
Southern	252	2.3	0.3	51.4	26.3	14.6
Arctic	698	2.1	0.4	26.5	20.1	17.7
Global	13398	116.9	28.7	2101.9	13.7	24.6

[a]Results are shown for major climate zones of the world and the global total.

for global forests. Global mean N deposition rates of 5.2 kg N ha^{-1} yr^{-1} [*Lamarque et al.*, 2010] would thus sequester 0.46 Pg C yr^{-1} in biomass. Global forest C sink strength was estimated at 2.4 ± 0.4 Pg C yr^{-1} (1990–2007) [*Pan et al.*, 2011], including both biomass and soil C pools. Given our simple accounting method, N deposition would sustain 19 ± 29% of the recent global forest C sink through effects on biomass production alone (Table 4). This additional C sink due to N deposition amounted to 0.07 ± 0.04 Pg C yr^{-1} in boreal, 0.11 ± 0.06 Pg C yr^{-1} in temperate, and 0.26 ± 0.17 Pg C yr^{-1} in tropical forest biomass, which is equivalent to 14 ± 4%, 16 ± 6%, and 23 ± 20% of the total forest C sink in these biomes, respectively (Table 4).

Based on global simulations, we derived a historical cumulative terrestrial C sink of 117 Pg C since 1900 (CN-Ac-G in Table 5). The tropics sequestered almost half (54.1 Pg C), followed by the temperate zone (31.4 Pg C), boreal zone (17.7 Pg C), and subtropical zone (9.2 Pg C). The preindustrial run (CN-Pi-G) results in 88.1 Pg C sequestered; thus, 28.7 Pg C, or 24%, has been sequestered due to rising N deposition at a rate of 13.7 kg C kg N^{-1} (Table 5 and Figure 5). N deposition has induced the strongest C sink in the tropics (11.9 Pg C) and temperate zone (10.7 Pg C). Conversely, in boreal and subtropical climates, the N-induced C sink was relatively small, with 3.3 and 2.2 Pg C (Table 5 and Figure 5). The N effect was highly variable within climate zones and included regional negative N effects, which were most pronounced in the tropics (Figure 5). This is a result of simulated disturbance events, causing stochastically induced loss of biomass, which causes variable N effects at smaller scales. Since biomass C represents a larger fraction of total ecosystem C in the tropics compared to the boreal or temperate zone,

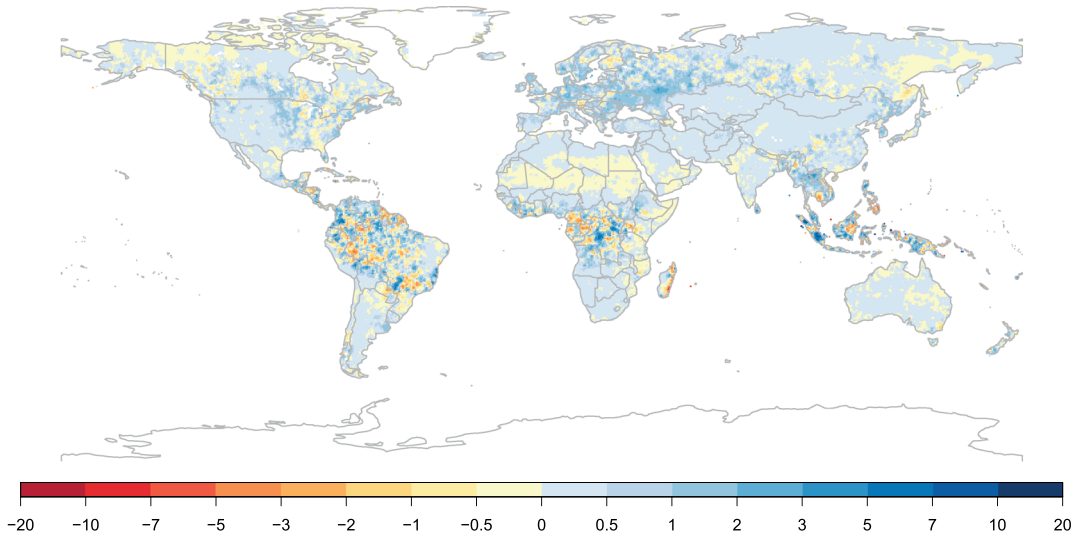

Figure 5. Ecosystem carbon accumulation from 1901 to 2006 due to rising N deposition, derived from total ecosystem C difference in 2006 between preindustrial and historical N deposition scenario simulations (ΔCN-Ac-G and CN-Pi-G) in kg C m^{-2}; positive values (blue) indicate a gain of C in ecosystems and negative values (red) a net C loss due to N deposition. Grid values were interpolated to derive a more coherent appearance.

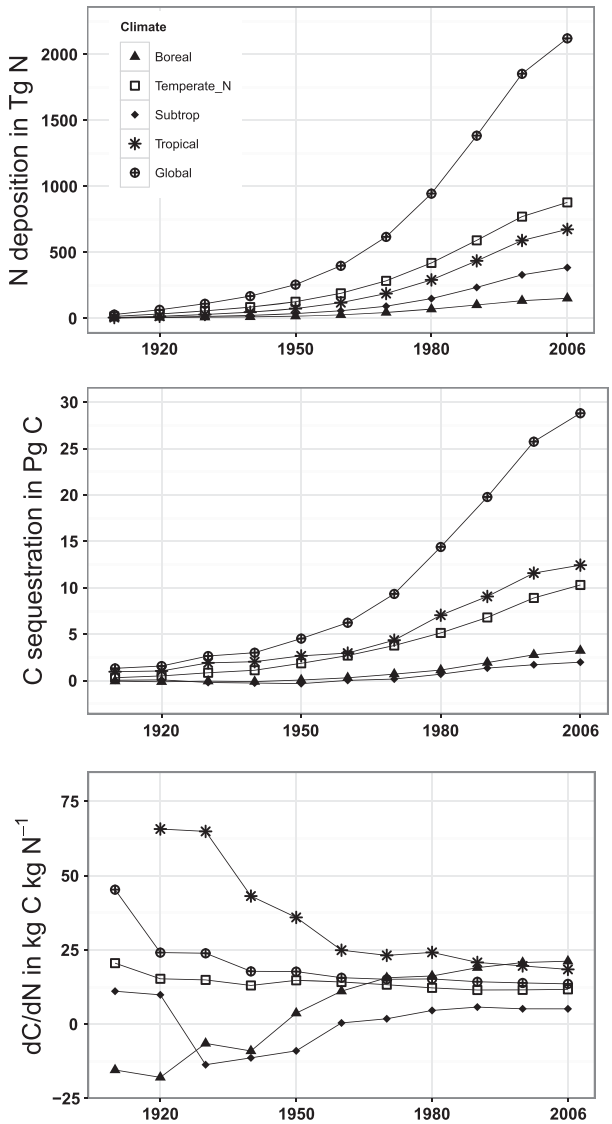

Figure 6. (top) Evolution of N deposition, (middle) N deposition-induced C sequestration, and (bottom) resulting dC/dN over the historical period, globally and per climate zone (see legend). N deposition as the cumulative difference between the preindustrial and historical N deposition scenario simulations (ΔCN-Ac-G and CN-Pi-G) in Tg N, N deposition-induced C sequestration as the difference in total ecosystem C pool between the two runs in Pg C, and the resulting dC/dN as C sequestration per N deposition in kg C kg N^{-1}. Results for a specified time cover the time period since 1900 until that point, e.g., 1980, assesses the period 1900–1980, etc. (calculating dC/dN per decade is not possible as initial states per decade differ between model runs). Note that the 1910 value for tropical is out of range (154 kg C kg N^{-1}).

these small-scale variations are more pronounced (see also Figure 3). These interactions point out the need to account for disturbances when assessing N effects at spatial scales where disturbances become relevant.

Temperate and tropical dC/dN from global simulations were 12 and 18 kg C kg N^{-1}, respectively, while boreal dC/dN was 22 kg C kg N^{-1} (Table 5), following the generally expected pattern of higher efficiencies in high latitudes. Boreal efficiencies are higher in the global simulation due to substantial sequestration of litter and soil C not accounted for in the site-scale simulations, while biomass dC/dN was comparable (Table S1 in the supporting information and Table 3). Boreal regions experience a positive N effect on C sequestration since 1950, with rising efficiencies since (Figure 6); however, the absolute effect of N deposition on C sequestration remained low. In contrast to boreal regions, biomass dC/dN was lower at global scale for tropical (13.7 versus 25.9 kg C kg N^{-1}) and temperate regions (7.6 versus 24.0 kg C kg N^{-1}) (Tables S1 and 3). Although global dC/dN was low for temperate and tropical ecosystems, substantial deposition of N induced considerable C sinks in these climate zones. This is despite temperate and tropical regions exhibiting signs of N saturation, as dC/dN moderately but steadily declines (Figure 6). While temperate and tropical regions received similar amounts of N, temperate N loads were highest on an area basis in both global and site simulations (Tables 3 and 5), supporting the likely onset of N saturation in this climate zone.

Another factor contributing to differences between site and global dC/dN are N deposition effects on PFT distribution. These play a role, as some spatial patterns in dC/dN were likely not captured by site simulations (Figure S1). For example, we observed increases in woody PFTs in Siberia (deciduous needleleaf forests, not shown) in the global simulations, for which no observational data from sites were available. The large presence of nonforest ecosystems (grasses) in the temperate zone explains partly lowered efficiency at a global scale, as the N deposition-induced stimulation of grass coverage (Figure S1) induces lower C sequestration compared to forests. Spatial shifts in PFTs due to CO_2 fertilization, N deposition, and climate have been assessed in more detail by *Wårlind et al.* [2014].

Table 6. Recent C Sequestration Rates and N Deposition Effects for 1990–2006 From Global Simulations, Mean C Sequestration (Pg C yr^{-1}), the Induced C Sequestration Due to N Deposition (Pg C yr^{-1}) (ΔCN-Ac-G and CN-Pi-G), Mean N Deposition (kg N ha^{-1} yr^{-1}) (CN-Ac-G), and the Contribution of N Deposition on Mean C Sequestration in Percent (N-Induced C Sink/C Sink)[a]

	C sink	N-Induced C Sink	N Deposition	N Deposition Effect
	Pg C yr^{-1}	Pg C yr^{-1}	kg N ha^{-1} yr^{-1}	%
Temperate (N)	0.75	0.22	6.97	29.12
Boreal	0.40	0.08	2.94	20.09
Tropical	1.46	0.21	4.68	14.41
Subtropical	0.21	0.04	5.20	18.46
Southern	0.07	0.00	1.50	5.07
Arctic	0.05	0.01	0.94	19.56
Global	2.95	0.56	4.57	19.11

[a]Results shown for major climate zones of the world and global totals.

To directly compare global simulations with the upscaling approach and observation-based estimates in *Pan et al*. [2011], we assess global simulation results for the time period 1990–2006 (Table 6). The simulated C uptake rates per climate zone agree well with observational-based estimates, e.g., 0.75 versus 0.72 Pg C yr^{-1} in the temperate zone and 0.40 versus 0.50 Pg C yr^{-1} in the boreal zone (Table 4). Global mean C sequestration (or NEE) was simulated at 2.95 Pg C yr^{-1} of which 0.56 Pg C yr^{-1} (or 19%) has been due to rising N deposition.

4. Discussion

The evaluation of LPJ-GUESS showed that the N cycle inclusion generally improved or equaled model performance of the C version. The extension of LPJ-GUESS with N cycle dynamics improved model predictions most notably for boreal evergreen needleleaf forests (BNE). Boreal forests were modeled with a greater degree of N limitation on GPP compared to temperate forests, in line with observations and modeling results [*Jarvis and Linder*, 2000; *Zaehle and Friend*, 2010; *Fleischer et al*., 2013]. The inclusion of the N cycle improved the simulation of both annual and seasonal GPPs of BNE when compared to the C version. In temperate forest ecosystems (TeNE and TeBS), effects of N dynamics were smaller and both model versions achieved comparable accuracies. The question is whether N limitation of temperate forests is in fact small or negligible, or whether it remains prevalent, but is compensated for by other processes and/or parameter settings in the C version. We believe the second is more likely, since experimental and monitoring studies indicate the prevalence of widespread N limitation in temperate forests, though there are examples of N saturation [*LeBauer and Treseder*, 2008; *Ferretti et al*., 2014]. Our modeled C sequestration responses to N deposition further support the hypothesis of enduring N limitation in temperate forests, although with moderate magnitude diminishing over time.

N dynamics in LPJ-GUESS induced changes in simulated ecosystem respiration and C pool sizes, both of which are linked due to the dependence of respiration on the stoichiometric composition of plant biomass and soil carbon. In the C version, C:N ratios are fixed for a given PFT and autotrophic respiration is entirely based on biomass C pool size, modified only by temperature. In the CN version, autotrophic respiration depends on flexible C:N ratios and N limitation realistically causes higher C:N ratios and lower respiration rates. Hence, the N cycle inclusion caused general reductions in R_{eco} and C pools, generally better matching observations, which is attributable to a combination of N controls on productivity and respiration. A moderate but persistent overestimation in R_{eco} remained however at the site scale in the CN version, especially for boreal and temperate deciduous forests (BNE and TeBS), hampering satisfactory predictions of NEE. Systematic overestimations of ecosystem respiration were not apparent previously [*Smith et al*., 2014] or in our global simulations (Table 5). Since biomass dynamics and N deposition effects have been modeled realistically at the site scale, the heterotrophic component of R_{eco} is likely contributing mainly to site-scale discrepancies. High soil C effluxes after disturbance often did not recover during the forests' lifetime to previous levels (not shown), which represents unrealistically long disturbance recovery times. The representation of respiratory processes in terrestrial models is hampered by the lack of adequate observations that broadly capture spatial and temporal variations, as well as competing but no superior modeling approach for soil C decomposition

to date [*Exbrayat et al*., 2013]. Furthermore, quantifying global C stocks [*Scharlemann et al*., 2014] and separating components of autotrophic and heterotrophic respiration as well as quantifying their interactions with environmental drivers and disturbances [*Exbrayat et al*., 2013] add challenging complexities to measuring and modeling respiration satisfactorily to date.

The model evaluation identified other remaining challenges for global ecosystem models. The unsatisfactory reproduction of C cycling in tropical forests by LPJ-GUESS is a feature generally shared by ecosystem models [*Castanho et al*., 2013]. This is inferred to be due to misrepresentations of plant and soil water-related mechanisms, identified earlier for LPJ-GUESS [*Morales et al*., 2005] and other ecosystem models [*Restrepo-Coupe et al*., 2013; *van der Molen et al*., 2011]. The accurate simulation of tropical ecosystem C and N cycles may notably be further complicated by the representation of such a diverse biome with commonly one or two PFTs, raising questions about the capability of ecosystem models in their current state to adequately capture tropical biogeochemical dynamics [*Pavlick et al*., 2013; *Van Bodegom et al*., 2012]. Another discrepancy between modeled and observed estimates was LAI, which did not satisfactorily match field observations for either version of LPJ-GUESS. This was rather unexpected as acceptable reproduction of forest LAI of LPJ-GUESS was reported earlier when compared to a different set of field observations [*Smith et al*., 2008]. Satisfactory prediction of C fluxes indicates that other model components might compensate for the underestimated amount of leaf area. The standard Beer's law light extinction coefficient (k) of 0.5 in LPJ-GUESS contributes to a low variation in LAI, leading to little additional increase in GPP above an LAI of 5 [see also *Jung et al*., 2007]. Model data agreement is further compromised by limited reliability of experimental observations and a lack of standardized methodologies across the FLUXNET network [*Bréda*, 2003].

The mean efficiency of converting deposited N into biomass amounted to 17.5 and 24 kg C kg N^{-1} in boreal and temperate forest sites, which are in the low to medium range when compared to the published range of 15 to 40 kg C kg N^{-1} from experimental and modeling studies [*De Vries et al*., 2009; in *Butterbach-Bahl et al*., 2011; *Erisman et al*., 2011]. Despite an expectation of strong N limitation in boreal forests, dC/dN was lowest for boreal site simulations. However, at global scale, efficiencies were highest for boreal regions (22 kg C kg N^{-1}), due to significant N-induced C sequestration in litter and soil C pools and due to increases in woody PFTs in some regions not captured by site simulations. For temperate regions on the other hand, efficiencies are actually lower at global scale (12 kg C kg N^{-1}) due to the onset of N saturation effects, as well as the consideration of disturbances and nonforest ecosystems, with generally less C sequestration potential [*Liu and Greaver*, 2009].

Despite diminishing efficiencies, in terms of actual N deposition-induced C sequestration, temperate forests provided a stronger recent and historical C sink than boreal forests based on our simulations and forest inventories [*Pan et al*., 2011]. Determining the onset and development of N saturation due to high N loads plays a key role in temperate forests [*Aber et al*., 1998; *Brumme and Khanna*, 2008]. While some studies have suggested signs of actual decline in C sink rates in temperate forests [*Nabuurs et al*., 2013], these were not severe in our simulation. Temperate forests remained substantial C sinks, and although relative N deposition effects slightly reduced, absolute effects remained considerable; i.e., there are limited signs of N saturation in temperate forests in our simulations.

Boreal ecosystems' C sequestration was limited to a net C uptake of 0.4–0.5 Pg C yr^{-1} in recent years (this study and also *Pan et al*. [2011]). N deposition was responsible for inducing 0.07–0.08 Pg C yr^{-1} thereof [*Pan et al*., 2011; this study; but also *Zaehle et al*., 2010]. Historically, this amounted to less than 3 Pg C, which is arguably small and corroborates conclusions by *Gundale et al*. [2014], arguing that the main N-induced C sink is not found in boreal forest. Although boreal forests (BNE) were most N limited in the model evaluation, their C response to N deposition was low at site scale and only moderate at global scale (when compared to the previous range of 15–40 kg C kg N^{-1}). Continuously low N deposition rates, combined with moderate efficiencies, prevented a substantial N-induced C sink. The rise of boreal dC/dN in recent decades might point toward stronger future effects of N deposition. However, we judge this to be of little relevance since predicted future N deposition loads in boreal regions are not expected to rise significantly [*Lamarque et al*., 2013; *Wårlind et al*., 2014]. Other processes such as a warming-induced higher soil N availability in boreal regions are believed to play a greater role than N deposition in terms of CN interactions relevant to the global C cycle [*Melillo et al*., 2011].

The large contribution of tropical regions to global C sequestration is apparent, since almost half of historical C sink has occurred in the tropics according to our simulations. Also, about half of the recent forest C sink is

attributed to the tropics, i.e., 1.19 of 2.40 Pg C yr^{-1} and 1.46 of 2.95 Pg C yr^{-1}, following forest inventories, and our simulations, respectively [*Pan et al*., 2011] (Table 4). Induced N limitation in the tropics was small (as hypothesized) in the site-scale model evaluation due to more favorable climate conditions for soil organic matter turnover and N mineralization [*Smith et al*., 2014]. Nonetheless, N deposition effects in our simulations were substantial in the tropics (26 and 18 kg C kg N^{-1} at site and global scales) with about one third of the N-induced C sequestration occurring in the tropics, which is in contrast to other similar modeling studies, e.g., *Zaehle et al*. [2010]. This strong simulated tropical N deposition effect in our study is however associated with greatest uncertainty given the unsatisfactory results during model evaluation, and the lack of P cycle dynamics, which are likely to further strongly control N effects and C dynamics in the tropics [*Cleveland et al*., 2011; *Vitousek et al*., 2010]. Thus, the N deposition effect might in reality be small or negligible, although positive responses to N fertilization [*LeBauer and Treseder*, 2008] have also been reported. The scarcity of relevant studies hampers a thorough evaluation in the tropics, where N effects are most uncertain [*Zaehle and Dalmonech*, 2011]. Nonetheless, the large amounts of N deposited over tropical forests worldwide and associated observed changes in tropical forests' N cycling [*Hietz et al*., 2011] call upon a careful evaluation of N deposition effects in these regions.

Furthermore, we have not accounted for deforestation and other land use and land cover changes (LULCCs), which have been estimated to bring net C balance of tropical forests close to zero due to C emissions from large-scale deforestation and fires [*Pan et al*., 2011]. Also, in temperate forests, the anthropogenic LULCC component is similarly central, as forest regrowth and management significantly determine the C balance [*Erb et al*., 2013; *Nabuurs et al*., 2013]. Interactions of N cycle and deposition with LULCC have so far been shown to mainly increase the net loss of C from ecosystems [*Gerber et al*., 2013; *Jain et al*., 2013] and thus are likely offsetting N deposition effects alone.

Globally, our accounting method based on site simulations indicated that 19 ± 29% of the recent global forest C sink, or 0.46 ± 0.28 Pg C yr^{-1}, is due to N deposition effects on biomass. The large uncertainties are mainly due to uncertainty of dC/dN and C sink strength in tropical forests. For boreal and temperate forests, the N deposition effect could be narrowed down to be within 10% to 22% (see Table 4). Our global simulations, representing spatial and temporal variability and including soil pools and other nonforest ecosystems, indicated a very comparable global N deposition effect of 0.56 Pg C yr^{-1}, representing 19% of the global C sink. Recent estimates of the N deposition effect on the global terrestrial C sink strength ranged from 0.2 to 0.4 Pg C yr^{-1} derived from global ecosystem model simulations [*Zaehle and Dalmonech*, 2011] and 0.4 to 0.6 Pg C yr^{-1} from a similar upscaling approach of field measurements [*Liu and Greaver*, 2009]. Our estimates of 0.46 and 0.56 Pg C yr^{-1} are thus in the medium to high end of these estimates, notably including a substantial N deposition effect in the tropics. Historically, our simulations indicate N deposition to be responsible for a sequestration of 0.26 Pg C yr^{-1} (1900–2006).

Assessing the response of global forest C sinks to N deposition remains of high priority due to expected changes in N deposition rates [*Lamarque et al*., 2013], remaining gaps in our understanding of relevant processes, and subsequent modeling deficiencies [*Zaehle and Dalmonech*, 2011]. Future experimental and monitoring efforts should be directed to underrepresented regions, such as the tropics or regions with high expected N inputs, e.g., temperate Asia [see *Lamarque et al*., 2013]. While most knowledge is derived from temperate ecosystems, it is evident that also there we are not completely confident in modeling CN interactions and they are a key contributor to global N effects; thus, efforts should not be lessened. Ecosystem models should further be rigorously tested with relevant measurements, ideally combining fluxes and pools of C and N, as well as P, a controlling factor with increasing importance not only in the tropics [*Peñuelas et al*., 2013]. Priorities should also be set to accurately represent processes governing N/P availability and limitation, such as N fixation, N/P uptake, and allocation, as well as interactions with LULCC in ecosystem models.

Appendix A: Text Box A1

The quantum efficiency scalar α_a controls CO_2 assimilation per unit photosynthetically active radiation absorbed, when scaling up from the leaf to the canopy level [*Tagesson et al*., 2009; *Smith et al*., 2014], and is highly influential on C flux and sequestration in LPJ-GUESS [*Zaehle et al*., 2005]. It was set at 0.7 for both

model versions. Previous standard LPJ-GUESS C version modeling efforts were based on more conservative estimates, e.g., 0.5 in *Haxeltine and Prentice* [1996], to force the global NPP to be within acceptable limits. However, this often caused an overestimation of primary productivity in boreal forests and an underestimation in temperate forests [*Morales et al.*, 2005; *Jung et al.*, 2007]. Previous settings of α_a were likely to compensate for the absence of N limitation, and the inclusion of the N cycle in the current study allows us to reproduce the gradient in productivity from temperate to boreal forests due to N cycle dynamics with a more realistic value of α_a of 0.7 [*Smith et al.*, 2014]. *Smith et al.* [2014], however, uses different settings of α_a, calibrated separately for the C and CN version to attain global C fluxes and stocks. While this produces realistic global predictions of both C and CN version, it does not allow extraction of the pure N cycle effect on predictions in LPJ-GUESS. For this reason, we have chosen a modeling setup in which C and CN version only differ in their inclusion, or exclusion, of the N cycle.

Table A1. List of FLUXNET Sites Included in Analysis ($n = 68$): Name and FLUXNET Abbreviation, Latitude, Year of Last Disturbance Used as Model Input, IGBP-Biome Classification [*Loveland et al.*, 2000] and Climate [*Kottek et al.*, 2006] According to FLUXNET, PFT Classification Used as Model Input for LPJ-GUESS, and Reference

Site	Name	Latitude	Distur.	IGBP	Climate	PFT	Reference[a]
BE-Bra	De Inslag Forest	51.31	1930	MF	TE	MF	*Janssens et al.* [1999]
BE-Vie	Vielsalm	50.31	1910	MF	TE	MF	*Aubinet et al.* [2001]
BR-Ban	Ecotone Bananal Island	−9.82	0	EBF	TR	TrBE	*da Rocha et al.* [2009]
BR-Ji2	Rebio Jara Ji Parana	−10.08	0	EBF	TR	TrBE	*von Randow et al.* [2004]
BR-Sa1	Santarem km67	−2.86	0	EBF	TR	TrBE	*Saleska et al.* [2003]
BR-Sa3	Santarem km83	−3.02	0	EBF	TR	TrBE	*Saleska et al.* [2003]
CA-Ca1	Campbell River, Mature	49.87	1950	ENF	TE	BNE	*Humphreys et al.* [2006]
CA-Ca2	Campbell River, Clearcut	49.87	1999	ENF	TE	BNE	*Humphreys et al.* [2006]
CA-Ca3	Campbell River, Young	49.53	1988	ENF	TE	BNE	*Humphreys et al.* [2006]
CA-Man	BOREAS NSA	55.88	1850	ENF	BO	BNE	*Dunn et al.* [2007]
CA-NS1	UCI 1850 burn site	55.88	1850	ENF	BO	BNE	*Goulden et al.* [2006]
CA-NS2	UCI 1930 burn site	55.91	1930	ENF	BO	BNE	*Goulden et al.* [2006]
CA-NS3	UCI 1964 burn site	55.91	1964	ENF	BO	BNE	*Goulden et al.* [2006]
CA-NS4	UCI 1964 burn site wet	55.91	1964	ENF	BO	BNE	Mike Goulden
CA-NS5	UCI 1981 burn site	55.86	1981	ENF	BO	BNE	*Goulden et al.* [2006]
CA-Obs	Sask. SSA Old Black Spr.	53.99	1870	ENF	BO	BNE	*Griffis et al.* [2003]
CA-Ojp	Sask. SSA Old Jack Pine	53.92	1920	ENF	BO	BNE	*Griffis et al.* [2003]
CA-Qcu	Quebec Cutover Boreal	49.27	2000	ENF	BO	BNE	*Giasson et al.* [2006]
CA-Qfo	Quebec Mature Boreal	49.69	1910	ENF	BO	BNE	*Bergeron et al.* [2007]
CA-SJ2	Sask. Harvest 2002	53.94	2002	ENF	BO	BNE	*Coursolle et al.* [2006]
CA-TP4	Turkey Point Mature	42.71	1939	ENF	TC	BNE	*Arain and Restrepo-Coupe* [2005]
CA-WP1	Western Peatland	54.95	1950	MF	BO	MF	*Flanagan and Syed* [2011]
CN-Cha	Changbaishan	42.4	1800	MF	TC	MF	*Guan et al.* [2006]
CZ-BK1	Bily Kriz	49.5	1980	ENF	TC	BNE	*Reichstein et al.* [2005]
DE-Bay	Bayreuth	50.14	1945	ENF	TE	BNE	*Staudt and Foken* [2007]
DE-Hai	Hainich	51.08	1750	DBF	TE	TeBS	*Knohl et al.* [2003]
DE-Har	Hartheim	47.93	1960	ENF	TE	TeNE	*Schindler et al.* [2006]
DE-Tha	Tharandt	50.96	1887	ENF	TE	TeNE	*Grünwald and Bernhofer* [2007]
DE-Wet	Wetzstein	50.45	1950	ENF	TE	BNE	*Anthoni et al.* [2004]
DK-Sor	Soroe	55.49	1920	DBF	TE	TeBS	*Pilegaard et al.* [2003]
ES-ES1	El Saler	39.35	1900	ENF	SM	TeNE	*Sanz et al.* [2004]
FI-Hyy	Hyytiala	61.85	1960	ENF	BO	BNE	*Vesala et al.* [2005]
FI-Sod	Sodankyla	67.36	1925	ENF	BO	BNE	*Suni et al.* [2003]
FR-Fon	Fontainebleau	48.48	1860	DBF	TE	TeBS	*Michelot et al.* [2011]
FR-Hes	Hesse Forest	48.67	1965	DBF	TE	TeBS	*Granier et al.* [2002]
FR-LBr	Le Bray	44.72	1970	ENF	TE	TeNE	*Berbigier et al.* [2001]
GF-Guy	French Guyana	5.28	1800	EBF	TR	TrBE	*Bonal et al.* [2008]
ID-Pag	Palangkaraya	2.35	1950	EBF	TR	TrBE	*Hirano et al.* [2007]
IL-Yat	Yatir	31.34	1965	ENF	DR	TeNE	*Grünzweig et al.* [2003]
IT-Lav	Lavarone	45.96	1920	ENF	TE	BNE	*Marcolla et al.* [2003]
IT-Non	Nonantola	44.69	1992	DBF	SM	TeBS	*Grassi and Magnani* [2005]
IT-PT1	Zerbolo-Parco Ticino-Canarazzo	45.2	1990	DBF	SM	TeBS	*Migliavacca et al.* [2009]
IT-Ren	Renon	46.59	1820	ENF	TE	BNE	*Montagnani et al.* [2009]
IT-SRo	San Rossore	43.73	1950	ENF	SM	TeNE	*Chiesi et al.* [2005]
IT-Vig	Vigevano	45.32	1990	DBF	SM	TeBS	*Zenone* [2007]

Table A1. (continued)

Site	Name	Latitude	Distur.	IGBP	Climate	PFT	Reference[a]
JP-Tef	Teshio Exp Forest	45.06	1835	MF	TC	MF	*Takagi et al.* [2009]
JP-Tom	Tomakomai	42.74	1960	MF	TC	MF	*Hirano et al.* [2003]
NL-Loo	Loobos	52.17	1900	ENF	TE	TeNE	*Dolman et al.* [2002]
RU-Fyo	Fyedorovskoye	56.46	1850	ENF	TC	BNE	*Milyukova et al.* [2002]
SE-Fla	Flakaliden	64.11	1960	ENF	BO	BNE	*Roberntz* [2001]
UK-Gri	Griffin	56.61	1980	ENF	TE	BNE	*Medlyn et al.* [2005a]
UK-Ham	Hampshire	51.12	1940	DBF	TE	TeBS	*Read et al.* [2009]
US-Bar	Bartlett Exp. Forest	44.06	1880	DBF	TC	TeBS	*Ollinger and Smith* [2005]
US-Blo	Blodgett Forest	38.9	1990	ENF	SM	BNE	*Goldstein et al.* [2000]
US-Bn1	Bonanza Creek 1920 burn	63.92	1920	ENF	BO	BNE	*Liu et al.* [2005]
US-Ho1	Howland (main tower)	45.2	1895	ENF	TC	BNE	*Davidson et al.* [2006]
US-Ho2	Howland (west tower)	45.21	1895	ENF	TC	BNE	*Davidson et al.* [2006]
US-LPH	Little Prospect Hill	42.54	1955	DBF	TC	TeBS	*Davidson et al.* [2006]
US-Me3	Metolius second Young Aged	44.32	1987	ENF	SM	BNE	*Campbell and Law* [2005]
US-Me4	Metolius Old	44.5	1810	ENF	SM	BNE	*Law et al.* [2001]
US-MMS	Morgan Monroe State Forest	39.32	1925	DBF	SM	TeBS	*Schmid et al.* [2000]
US-MOz	Missouri Ozark	38.74	1930	DBF	SM	TeBS	*Gu et al.* [2006]
US-NC2	North Carolina Loblolly Pine	35.8	1992	ENF	SM	TeNE	*Noormets et al.* [2010]
US-NR1	Niwot Ridge Forest	40.03	1900	ENF	BO	BNE	*Monson et al.* [2002]
US-Oho	Oak Openings	41.55	1960	DBF	TC	TeBS	*DeForest et al.* [2006]
US-UMB	University Michigan Biological Station	45.56	1910	DBF	TC	TeBS	*Gough et al.* [2013]
US-Wcr	Willow Creek	45.81	1920	DBF	TC	TeBS	*Desai et al.* [2005]
US-Wrc	Wind River Crane	45.82	1550	ENF	TE	TeNE	*Chen et al.* [2004]

[a]Name of principal investigator was given if no site reference was available.

Acknowledgments
FLUXNET observations were obtained from the Oak Ridge National Laboratory Distributed Active Archive Center (ORNL DAAC), available online (http://fluxnet.ornl.gov) from ORNL DAAC, Oak Ridge, Tennessee, USA. FLUXNET data used in this study are in parts open access, whereas parts are restricted to data contributors. Derivation of data and modeling products is described in the paper and available upon request. We thank all the scientists involved in the continuous collection of FLUXNET measurements and maintaining the data sets, which made this study possible. The eddy covariance data were acquired by the FLUXNET community and in particular by the following networks: AmeriFlux (U.S. Department of Energy, Biological and Environmental Research, Terrestrial Carbon Program, DE-FG02-04ER63917 and DE-FG02-04ER63911), AsiaFlux, CarboEuropeIP, ChinaFlux, Fluxnet-Canada Research Network (supported by CFCAS, NSERC, BIOCAP, Environment Canada, and NRCan), LBA, and OzFlux. We acknowledge the financial support to the eddy covariance data harmonization provided by CarboEuropeIP, FAO-GTOS-TCO, iLEAPS, Max Planck Institute for Biogeochemistry, National Science Foundation, University of Tuscia, Université Laval, Environment Canada, and the U.S. Department of Energy and the database development and technical support from Berkeley Water Center, Lawrence Berkeley National Laboratory, Microsoft Research eScience,

References

Aber, J., W. McDowell, K. Nadelhoffer, A. Magill, G. Berntson, M. Kamakea, S. McNulty, W. Currie, L. Rustad, and I. Fernandez (1998), Nitrogen saturation in temperate forest ecosystems—Hypotheses revisited, *BioScience*, *48*(11), 921–934.

Ahlström, A., G. Schurgers, A. Arneth, and B. Smith (2012), Robustness and uncertainty in terrestrial ecosystem carbon response to CMIP5 climate change projections, *Environ. Res. Lett.*, *7*(4), 044008.

Anthoni, P. M., A. Knohl, C. Rebmann, A. Freibauer, M. Mund, W. Ziegler, O. Kolle, and E.-D. Schulze (2004), Forest and agricultural land-use-dependent CO_2 exchange in Thuringia, Germany, *Global Change Biol.*, *10*(12), 2005–2019, doi:10.1111/j.1365-2486.2004.00863.x.

Arain, M. A., and N. Restrepo-Coupe (2005), Net ecosystem production in a temperate pine plantation in southeastern Canada, *Agric. For. Meteorol.*, *128*(3–4), 223–241.

Arneth, A., et al. (2010), Terrestrial biogeochemical feedbacks in the climate system, *Nat. Geosci.*, *3*(8), 525–532, doi:10.1038/ngeo905.

Aubinet, M., B. Chermanne, M. Vandenhaute, B. Longdoz, M. Yernaux, and E. Laitat (2001), Long term carbon dioxide exchange above a mixed forest in the Belgian Ardennes, *Agric. For. Meteorol.*, *108*(4), 293–315, doi:10.1016/S0168-1923(01)00244-1.

Baldocchi, D., et al. (2001), FLUXNET: A new tool to study the temporal and spatial variability of ecosystem-scale carbon dioxide, water vapor, and energy flux densities, *Bull. Am. Meteorol. Soc.*, *82*(11), 2415–2434.

Berbigier, P., J.-M. Bonnefond, and P. Mellmann (2001), CO_2 and water vapour fluxes for 2 years above Euroflux forest site, *Agric. For. Meteorol.*, *108*(3), 183–197, doi:10.1016/S0168-1923(01)00240-4.

Bergeron, O., H. A. Margolis, T. A. Black, C. Coursolle, A. L. Dunn, A. G. Barr, and S. C. Wofsy (2007), Comparison of carbon dioxide fluxes over three boreal black spruce forests in Canada, *Global Change Biol.*, *13*(1), 89–107, doi:10.1111/j.1365-2486.2006.01281.x.

Bonal, D., et al. (2008), Impact of severe dry season on net ecosystem exchange in the Neotropical rainforest of French Guiana, *Global Change Biol.*, *14*(8), 1917–1933, doi:10.1111/j.1365-2486.2008.01610.x.

Bréda, N. J. J. (2003), Ground-based measurements of leaf area index: A review of methods, instruments and current controversies, *J. Exp. Bot.*, *54*(392), 2403–2417, doi:10.1093/jxb/erg263.

Brumme, R., and P. K. Khanna (2008), Ecological and site historical aspects of N dynamics and current N status in temperate forests, *Global Change Biol.*, *14*(1), 125–141, doi:10.1111/j.1365-2486.2007.01460.x.

Butterbach-Bahl, K., E. Nemitz, and S. Zaehle (2011), Nitrogen as a threat to the European greenhouse balance, in *The European Nitrogen Assessment*, edited by M. Sutton, pp. 434–462, Cambridge Univ. Press, Cambridge, U. K.

Campbell, J., and B. Law (2005), Forest soil respiration across three climatically distinct chronosequences in Oregon, *Biogeochemistry*, *73*(1), 109–125, doi:10.1007/s10533-004-5165-9.

Castanho, A. D. A., M. T. Coe, M. H. Costa, Y. Malhi, D. Galbraith, and C. A. Quesada (2013), Improving simulated Amazon forest biomass and productivity by including spatial variation in biophysical parameters, *Biogeosciences*, *10*(4), 2255–2272, doi:10.5194/bg-10-2255-2013.

Chen, J., K. T. Paw U, S. L. Ustin, T. H. Suchanek, B. J. Bond, K. D. Brosofske, and M. Falk (2004), Net ecosystem exchanges of carbon, water, and energy in young and old-growth Douglas-fir forests, *Ecosystems*, *7*, 534–544, doi:10.1007/s10021-004-0143-.

Chiesi, M., F. Maselli, M. Bindi, L. Fibbi, P. Cherubini, E. Arlotta, G. Tirone, G. Matteucci, and G. Seufert (2005), Modelling carbon budget of Mediterranean forests using ground and remote sensing measurements, *Agric. For. Meteorol.*, *135*(1–4), 22–34, doi:10.1016/j.agrformet.2005.09.011.

Churkina, G., S. Zaehle, J. Hughes, N. Viovy, Y. Chen, M. Jung, B. W. Heumann, N. Ramankutty, M. Heimann, and C. Jones (2010), Interactions between nitrogen deposition, land cover conversion, and climate change determine the contemporary carbon balance of Europe, *Biogeosci. Discuss.*, *7*(2), 2227–2265, doi:10.5194/bgd-7-2227-2010.

Oak Ridge National Laboratory, University of California-Berkeley, and University of Virginia. We acknowledge NWO for providing a PhD grant (NWO 829.09.006) enabling the research to be carried out by Katrin Fleischer. David Wårlind and Almut Arneth acknowledge support from the Formas Strong Research Environment "Land use today and tomorrow" and the EU FP7 project ECLAIRE (grant 282910).

Cleveland, C. C., et al. (1999), Global patterns of terrestrial biological nitrogen (N2) fixation in natural ecosystems, *Global Biogeochem. Cycles*, *13*(2), 623–645, doi:10.1029/1999GB900014.

Cleveland, C. C., et al. (2011), Relationships among net primary productivity, nutrients and climate in tropical rain forest: A pan-tropical analysis, *Ecol. Lett.*, *14*(9), 939–947, doi:10.1111/j.1461-0248.2011.01658.x.

Coursolle, C., et al. (2006), Late-summer carbon fluxes from Canadian forests and peatlands along an eastwest continental transect, *Can. J. For. Res.*, *36*(3), 783–800.

da Rocha, H. R., et al. (2009), Patterns of water and heat flux across a biome gradient from tropical forest to savanna in Brazil, *J. Geophys. Res.*, *114*, G00B12, doi:10.1029/2007JG000640.

Davidson, E. A., K. E. Savage, S. E. Trumbore, and W. Borken (2006), Vertical partitioning of CO_2 production within a temperate forest soil, *Global Change Biol.*, *12*(6), 944–956, doi:10.1111/j.1365-2486.2005.01142.x.

DeForest, J., A. Noormets, S. McNulty, G. Sun, G. Tenney, and J. Chen (2006), Phenophases alter the soil respiration-temperature relationship in an oak-dominated forest, *Int. J. Biometeorol.*, *51*, 135–144, doi:10.1007/s00484-006-0046-7.

Dentener, F., et al. (2006), Nitrogen and sulfur deposition on regional and global scales: A multimodel evaluation, *Global Biogeochem. Cycles*, *20*, GB4003, doi:10.1029/2005GB002672.

Desai, A. R., P. V. Bolstad, B. D. Cook, K. J. Davis, and E. V. Carey (2005), Comparing net ecosystem exchange of carbon dioxide between an old-growth and mature forest in the upper Midwest, USA, *Agric. For. Meteorol.*, *128*(1–2), 33–55, doi:10.1016/j.agrformet.2004.09.005.

de Vries, W., et al. (2009), The impact of nitrogen deposition on carbon sequestration by European forests and heathlands, *For. Ecol. Manage.*, *258*(8), 1814–1823, doi:10.1016/j.foreco.2009.02.034.

Dolman, A. J., E. J. Moors, and J. A. Elbers (2002), The carbon uptake of a mid latitude pine forest growing on sandy soil, *Agric. For. Meteorol.*, *111*(3), 157–170, doi:10.1016/S0168-1923(02)00024-2.

Dunn, A. L., C. C. Barford, S. C. Wofsy, M. L. Goulden, and B. C. Daube (2007), A long-term record of carbon exchange in a boreal black spruce forest: Means, responses to interannual variability, and decadal trends, *Global Change Biol.*, *13*(3), 577–590, doi:10.1111/j.1365-2486.2006.01221.x.

Erb, K., T. Kastner, S. Luyssaert, R. Houghton, T. Kuemmerle, P. Olofsson, and H. Haberl (2013), Bias in the attribution of forest carbon sinks, *Nat. Clim. Change*, *3*, 854–856.

Erisman, J. W., J. Galloway, S. Seitzinger, A. Bleeker, and K. Butterbach-Bahl (2011), Reactive nitrogen in the environment and its effect on climate change, *Curr. Opin. Environ. Sustainability*, *3*(5), 281–290, doi:10.1016/j.cosust.2011.08.012.

Esser, G., J. Kattge, and A. Sakalli (2011), Feedback of carbon and nitrogen cycles enhances carbon sequestration in the terrestrial biosphere, *Global Change Biol.*, *17*(2), 819–842, doi:10.1111/j.1365-2486.2010.02261.x.

Exbrayat, J.-F., A. J. Pitman, G. Abramowitz, and Y.-P. Wang (2013), Sensitivity of net ecosystem exchange and heterotrophic respiration to parameterization uncertainty, *J. Geophys. Res. Atmos.*, *118*, 1640–1651, doi:10.1029/2012JD018122.

FAO/IIASA/ISRIC/ISSCAS/JRC (2012), Harmonized World Soil Database (version 1.2), FAO, Rome, Italy and IIASA, Laxenburg, Austria. Accessed: 27 November, 2014.

Ferretti, M., et al. (2014), On the tracks of nitrogen deposition effects on temperate forests at their southern European range—An observational study from Italy, *Global Change Biol.*, doi:10.1111/gcb.12552, in press.

Field, C., and H. A. Mooney (1986), The photosynthesis-nitrogen relationship in wild plants, in *On the Economy of Plant Form and Function: Adaptive Patterns of Energy Capture in Plants*, edited by T. J. Givnish, pp. 25–56, Cambridge Univ. Press, Cambridge, U. K.

Fisher, J. B., G. Badgley, and E. Blyth (2012), Global nutrient limitation in terrestrial vegetation, *Global Biogeochem. Cycles*, *26*, GB3007, doi:10.1029/2011GB004252.

Flanagan, L. B., and K. H. Syed (2011), Stimulation of both photosynthesis and respiration in response to warmer and drier conditions in a boreal peatland ecosystem, *Global Change Biol.*, *17*(7), 2271–2287, doi:10.1111/j.1365-2486.2010.02378.x.

Fleischer, K., et al. (2013), The contribution of nitrogen deposition to the photosynthetic capacity of forests, *Global Biogeochem. Cycles*, *27*, 1–13, doi:10.1002/gbc.20026.

Friend, A. D., et al. (2007), FLUXNET and modelling the global carbon cycle, *Global Change Biol.*, *13*(3), 610–633, doi:10.1111/j.1365-2486.2006.01223.x.

Galloway, J., J. Aber, J. Erisman, S. Seitzinger, R. Howarth, E. Cowling, and B. Cosby (2003), The nitrogen cascade, *BioScience*, *53*(4), 341–356.

Galloway, J. N., A. R. Townsend, J. W. Erisman, M. Bekunda, Z. Cai, J. R. Freney, L. A. Martinelli, S. P. Seitzinger, and M. A. Sutton (2008), Transformation of the nitrogen cycle: Recent trends, questions, and potential solutions, *Science*, *320*(5878), 889–892, doi:10.1126/science.1136674.

Gerber, S., L. O. Hedin, S. G. Keel, S. W. Pacala, and E. Shevliakova (2013), Land use change and nitrogen feedbacks constrain the trajectory of the land carbon sink, *Geophys. Res. Lett.*, *40*, 5218–5222, doi:10.1002/grl.50957.

Giasson, M.-A., C. Coursolle, and H. A. Margolis (2006), Ecosystem-level CO_2 fluxes from a boreal cutover in eastern Canada before and after scarification, *Agric. For. Meteorol.*, *140*, 23–40, doi:10.1016/j.agrformet.2006.08.001.

Goldstein, A., N. Hultman, J. Fracheboud, M. Bauer, J. Panek, M. Xu, Y. Qi, A. Guenther, and W. Baugh (2000), Effects of climate variability on the carbon dioxide, water, and sensible heat fluxes above a ponderosa pine plantation in the Sierra Nevada (CA), *Agric. For. Meteorol.*, *101*, 113–129, doi:10.1016/S0168-1923(99)00168-9.

Gough, C. M., B. S. Hardiman, L. E. Nave, G. Bohrer, K. D. Maurer, C. S. Vogel, K. J. Nadelhoffer, and P. S. Curtis (2013), Sustained carbon uptake and storage following moderate disturbance in a Great Lakes forest, *Ecol. Appl.*, *23*(5), 1202–1215, doi:10.1890/12-1554.1.

Goulden, M. L., G. C. Winston, A. M. S. McMillan, M. E. Litvak, E. L. Read, A. V. Rocha, and J. R. Elliot (2006), An eddy covariance mesonet to measure the effect of forest age on land-atmosphere exchange, *Global Change Biol.*, *12*(11), 2146–2162, doi:10.1111/j.1365-2486.2006.01251.x.

Granier, A., K. Pilegaard, and N. O. Jensen (2002), Similar net ecosystem exchange of beech stands located in France and Denmark, *Agric. For. Meteorol.*, *114*(1–2), 75–82, doi:10.1016/S0168-1923(02)00137-5.

Grassi, G., and F. Magnani (2005), Stomatal, mesophyll conductance and biochemical limitations to photosynthesis as affected by drought and leaf ontogeny in ash and oak trees, *Plant, Cell Environ.*, *28*(7), 834–849, doi:10.1111/j.1365-3040.2005.01333.x.

Griffis, T. J., T. A. Black, K. Morgenstern, A. G. Barr, Z. Nesic, G. B. Drewitt, D. Gaumont-Guay, and J. H. McCaughey (2003), Ecophysiological controls on the carbon balances of three southern boreal forests, *Agric. For. Meteorol.*, *117*(1–2), 53–71, doi:10.1016/S0168-1923(03)00023-6.

Gruber, N., and J. N. Galloway (2008), An Earth-system perspective of the global nitrogen cycle, *Nature*, *451*(7176), 293–296.

Grünwald, T., and C. Bernhofer (2007), A decade of carbon, water and energy flux measurements of an old spruce forest at the Anchor Station Tharandt, *Tellus B*, *59*(3), 387–396, doi:10.1111/j.1600-0889.2007.00259.x.

Grünzweig, J., T. Lin, E. Rotenberg, A. Schwartz, and D. Yakir (2003), Carbon sequestration in arid-land forest, *Global Change Biol.*, *9*(5), 791–799.

Gu, L., T. Meyers, S. G. Pallardy, P. J. Hanson, B. Yang, M. Heuer, K. P. Hosman, J. S. Riggs, D. Sluss, and S. D. Wullschleger (2006), Direct and indirect effects of atmospheric conditions and soil moisture on surface energy partitioning revealed by a prolonged drought at a temperate forest site, *J. Geophys. Res.*, *111*, D16102, doi:10.1029/2006JD007161.

Guan, D.-X., J.-B. Wu, X.-S. Zhao, S.-J. Han, G.-R. Yu, X.-M. Sun, and C.-J. Jin (2006), CO_2 fluxes over an old, temperate mixed forest in northeastern China, *Agric. For. Meteorol.*, *137*(3–4), 138–149.

Gundale, M. J., F. From, L. H. Bach, and A. Nordin (2014), Anthropogenic nitrogen deposition in boreal forests has a minor impact on the global carbon cycle, *Global Change Biol.*, *20*(1), 276–286, doi:10.1111/gcb.12422.

Haxeltine, A., and I. Prentice (1996), A general model for the light-use efficiency of primary production, *Funct. Ecol.*, *10*(5), 551–561.

Hickler, T., B. Smith, I. C. Prentice, K. Mjöfors, P. Miller, A. Arneth, and M. T. Sykes (2008), CO_2 fertilization in temperate FACE experiments not representative of boreal and tropical forests, *Global Change Biol.*, *14*(7), 1531–1542, doi:10.1111/j.1365-2486.2008.01598.x.

Hickler, T., et al. (2012), Projecting the future distribution of European potential natural vegetation zones with a generalized, tree species-based dynamic vegetation model, *Global Ecol. Biogeogr.*, *21*(1), 50–63, doi:10.1111/j.1466-8238.2010.00613.x.

Hietz, P., B. L. Turner, W. Wanek, A. Richter, C. A. Nock, and S. J. Wright (2011), Long-term change in the nitrogen cycle of tropical forests, *Science*, *334*(6056), 664–666, doi:10.1126/science.1211979.

Hirano, T., R. Hirata, Y. Fujinuma, N. Saigusa, S. Yamamoto, Y. Harazono, M. Takada, K. Inukai, and G. Inoue (2003), CO_2 and water vapor exchange of a larch forest in northern Japan, *Tellus B*, *55*(2), 244–257.

Hirano, T., H. Segah, T. Harada, S. Limin, T. June, R. Hirata, and M. Osaki (2007), Carbon dioxide balance of a tropical peat swamp forest in Kalimantan, Indonesia, *Global Change Biol.*, *13*(2), 412–425, doi:10.1111/j.1365-2486.2006.01301.x.

Högberg, P. (2011), What is the quantitative relation between nitrogen deposition and forest carbon sequestration?, *Global Change Biol.*, *18*, 1–2, doi:10.1111/j.1365-2486.2011.02553.x.

Humphreys, E. R., T. A. Black, K. Morgenstern, T. Cai, G. B. Drewitt, Z. Nesic, and J. Trofymow (2006), Carbon dioxide fluxes in coastal Douglas-fir stands at different stages of development after clearcut harvesting, *Agric. For. Meteorol.*, *140*(1–4), 6–22, doi:10.1016/j.agrformet.2006.03.018.

Jain, A., X. Yang, H. Kheshgi, A. D. McGuire, W. Post, and D. Kicklighter (2009), Nitrogen attenuation of terrestrial carbon cycle response to global environmental factors, *Global Biogeochem. Cycles*, *23*, GB4028, doi:10.1029/2009GB003519.

Jain, A. K., P. Meiyappan, Y. Song, and J. I. House (2013), CO_2 emissions from land-use change affected more by nitrogen cycle, than by the choice of land-cover data, *Global Change Biol.*, *19*(9), 2893–2906, doi:10.1111/gcb.12207.

Janssens, I. A., and S. Luyssaert (2009), Carbon cycle: Nitrogen's carbon bonus, *Nat. Geosci.*, *2*(5), 318–319, doi:10.1038/ngeo505.

Janssens, I. A., D. A. Sampson, J. Cermak, L. Meiresonne, F. Riguzzi, S. Overloop, and R. Ceulemans (1999), Above- and belowground phytomass and carbon storage in a Belgian Scots pine stand, *Ann. For. Sci.*, *56*(2), 81–90, doi:10.1051/forest:19990201.

Jarvis, P., and S. Linder (2000), Botany: Constraints to growth of boreal forests, *Nature*, *405*(6789), 904–905, doi:10.1038/35016154.

Jung, M., G. Le Maire, S. Zaehle, S. Luyssaert, M. Vetter, G. Churkina, P. Ciais, N. Viovy, and M. Reichstein (2007), Assessing the ability of three land ecosystem models to simulate gross carbon uptake of forests from boreal to Mediterranean climate in Europe, *Biogeosciences*, *4*(4), 647–656, doi:10.5194/bg-4-647-2007.

Kergoat, L., S. Lafont, A. Arneth, V. Le Dantec, and B. Saugier (2008), Nitrogen controls plant canopy light-use efficiency in temperate and boreal ecosystems, *J. Geophys. Res.*, *113*, G04017, doi:10.1029/2007JG000676.

Knohl, A., E.-D. Schulze, O. Kolle, and N. Buchmann (2003), Large carbon uptake by an unmanaged 250-year-old deciduous forest in Central Germany, *Agric. For. Meteorol.*, *118*(3–4), 151–167.

Kottek, M., J. Grieser, C. Beck, B. Rudolf, and F. Rubel (2006), World Map of the Köppen-Geiger climate classification updated, *Meteorol. Z.*, *15*, 259–263, doi:10.1127/0941-2948/2006/0130.

Lamarque, J.-F., et al. (2010), Historical (1850–2000) gridded anthropogenic and biomass burning emissions of reactive gases and aerosols: Methodology and application, *Atmos. Chem. Phys.*, *10*(15), 7017–7039, doi:10.5194/acp-10-7017-2010.

Lamarque, J.-F., et al. (2013), Multi-model mean nitrogen and sulfur deposition from the Atmospheric Chemistry and Climate Model Intercomparison Project (ACCMIP): Evaluation of historical and projected future changes, *Atmos. Chem. Phys.*, *13*(16), 7997–8018, doi:10.5194/acp-13-7997-2013.

Law, B., P. Thornton, J. Irvine, P. Anthoni, and S. Van Tuyl (2001), Carbon storage and fluxes in ponderosa pine forests at different developmental stages, *Global Change Biol.*, *7*(7), 755–777.

Lawrence, P. J., et al. (2012), Simulating the biogeochemical and biogeophysical impacts of transient land cover change and wood harvest in the Community Climate System Model (CCSM4) from 1850 to 2100, *J. Clim.*, *25*(9), 3071–3095, doi:10.1175/JCLI-D-11-00256.1.

LeBauer, D. S., and K. K. Treseder (2008), Nitrogen limitation of net primary productivity in terrestrial ecosystems is globally distributed, *Ecology*, *89*(2), 371–379.

Le Quéré, C., et al. (2013), The global carbon budget 1959–2011, *Earth Syst. Sci. Data*, *5*(1), 165–185, doi:10.5194/essd-5-165-2013.

Liu, H., J. T. Randerson, J. Lindfors, I. Chapin, and F. Stuart (2005), Changes in the surface energy budget after fire in boreal ecosystems of interior Alaska: An annual perspective, *J. Geophys. Res.*, *110*, D13101, doi:10.1029/2004JD005158.

Liu, L., and T. L. Greaver (2009), A review of nitrogen enrichment effects on three biogenic GHGs: The CO_2 sink may be largely offset by stimulated N_2O and CH_4 emission, *Ecol. Lett.*, *12*(10), 1103–1117, doi:10.1111/j.1461-0248.2009.01351.x.

Loveland, T. R., B. C. Reed, J. F. Brown, D. O. Ohlen, Z. Zhu, L. Yang, and J. W. Merchant (2000), Development of a global land cover characteristics database and IGBP DISCover from 1 km AVHRR data, *Int. J. Remote Sens.*, *21*, 1303–1330.

Luysseart, S., et al. (2007), CO_2 balance of boreal, temperate, and tropical forests derived from a global database, *Global Change Biol.*, *13*(12), 2509–2537, doi:10.1111/j.1365-2486.2007.01439.x.

Marcolla, B., A. Pitacco, and A. Cescatti (2003), Canopy architecture and turbulence structure in a coniferous forest, *Boundary Layer Meteorol.*, *108*(1), 39–59.

Maréchal, D. (2004), A soil-based approach to rainfall-runoff modelling in ungauged catchments for England and Wales, PhD thesis, Cranfield Univ.

Matear, R. J., Y.-P. Wang, and A. Lenton (2010), Land and ocean nutrient and carbon cycle interactions, *Curr. Opin. Environ. Sustainability*, *2*(4), 258–263, doi:10.1016/j.cosust.2010.05.009.

McGuire, A. D., et al. (2001), Carbon balance of the terrestrial biosphere in the twentieth century: Analyses of CO_2, climate and land use effects with four process-based ecosystem models, *Global Biogeochem. Cycles*, *15*(1), 183–206, doi:10.1029/2000GB001298.

Medlyn, B., A. Robinson, R. Clement, and R. McMurtrie (2005b), On the validation of models of forest CO_2 exchange using eddy covariance data: Some perils and pitfalls, *Tree Physiol.*, *25*(7), 839–857.

Medlyn, B. E., P. Berbigier, R. Clement, A. Grelle, D. Loustau, S. Linder, L. Wingate, P. G. Jarvis, B. D. Sigurdsson, and R. E. McMurtrie (2005a), Carbon balance of coniferous forests growing in contrasting climates: Model-based analysis, *Agric. For. Meteorol.*, *131*(1–2), 97–124, doi:10.1016/j.agrformet.2005.05.004.

Melillo, J. M., et al. (2011), Soil warming, carbon-nitrogen interactions, and forest carbon budgets, *Proc. Natl. Acad. Sci. U.S.A.*, *108*, 9508–9512, doi:10.1073/pnas.1018189108.

Michelot, A., T. Eglin, E. Dufrene, C. Lelarge-Trouverie, and C. Damesin (2011), Comparison of seasonal variations in water-use efficiency calculated from the carbon isotope composition of tree rings and flux data in a temperate forest, *Plant, Cell Environ.*, *34*(2), 230–244, doi:10.1111/j.1365-3040.2010.02238.x.

Migliavacca, M., et al. (2009), Seasonal and interannual patterns of carbon and water fluxes of a poplar plantation under peculiar eco-climatic conditions, *Agric. For. Meteorol.*, *149*(9), 1460–1476, doi:10.1016/j.agrformet.2009.04.003.

Milyukova, I., O. Kolle, A. Varlagin, N. Vygodskaya, E. Schulze, and J. Lloyd (2002), Carbon balance of a southern taiga spruce stand in European Russia, *Tellus B*, *54*(5), 429–442.

Mitchell, T. D., and P. D. Jones (2005), An improved method of constructing a database of monthly climate observations and associated high-resolution grids, *Int. J. Climatol.*, *25*(6), 693–712, doi:10.1002/joc.1181.

Monson, R. K., A. A. Turnipseed, J. P. Sparks, P. C. Harley, L. E. Scott-Denton, K. Sparks, and T. E. Huxman (2002), Carbon sequestration in a high-elevation, subalpine forest, *Global Change Biol.*, *8*(5), 459–478, doi:10.1046/j.1365-2486.2002.00480.x.

Montagnani, L., et al. (2009), A new mass conservation approach to the study of CO_2 advection in an alpine forest, *J. Geophys. Res.*, *114*, D07306, doi:10.1029/2008JD010650.

Morales, P., et al. (2005), Comparing and evaluating process-based ecosystem model predictions of carbon and water fluxes in major European forest biomes, *Global Change Biol.*, *11*(12), 2211–2233, doi:10.1111/j.1365-2486.2005.01036.x.

Nabuurs, G.-J., M. Lindner, P. Verkerk, K. Gunia, P. Deda, P. Michalak, and G. Grassi (2013), First signs of carbon sink saturation in European forest biomass, *Nat. Clim. Change*, *3*, 792–796.

Noormets, A., M. Gavazzi, S. McNulty, J.-C. Domec, G. Sun, J. King, and J. Chen (2010), Response of carbon fluxes to drought in a coastal plain loblolly pine forest, *Global Change Biol.*, *16*(1), 272–287, doi:10.1111/j.1365-2486.2009.01928.x.

Ollinger, S., and M.-L. Smith (2005), Net primary production and canopy nitrogen in a temperate forest landscape: An analysis using imaging spectroscopy, modeling and field data, *Ecosystems*, *8*, 760–778, doi:10.1007/s10021-005-0079-5.

Pan, Y., et al. (2011), A large and persistent carbon sink in the world's forests, *Science*, *333*(6045), 988–993, doi:10.1126/science.1201609.

Pavlick, R., D. T. Drewry, K. Bohn, B. Reu, and A. Kleidon (2013), The Jena Diversity-Dynamic Global Vegetation Model (JeDi-DGVM): A diverse approach to representing terrestrial biogeography and biogeochemistry based on plant functional trade-offs, *Biogeosciences*, *10*(6), 4137–4177, doi:10.5194/bg-10-4137-2013.

Peñuelas, J., et al. (2013), Human-induced nitrogen-phosphorus imbalances alter natural and managed ecosystems across the globe, *Nat. Commun.*, *4*, doi:10.1038/ncomms3934.

Pilegaard, K., T. Mikkelsen, C. Beier, N. Jensen, P. Ambus, and H. Ro-Poulsen (2003), Field measurements of atmosphere-biosphere interactions in a Danish beech forest, *Boreal Environ. Res.*, *8*(4), 315–333.

Read, D. J., P. H. Freer-Smith, J. I. L. Morison, N. Hanley, C. C. West, and P. Snowdon (2009), *Combating Climate Change—A Role for UK Forests. An Assessment of the Potential of the UK's Trees and Woodlands to Mitigate and Adapt to Climate Change*, p. 222, TSO, Edinburgh, U. K.

Reichstein, M., et al. (2005), On the separation of net ecosystem exchange into assimilation and ecosystem respiration: Review and improved algorithm, *Global Change Biol.*, *11*(9), 1424–1439, doi:10.1111/j.1365-2486.2005.001002.x.

Restrepo-Coupe, N., et al. (2013), What drives the seasonality of photosynthesis across the Amazon basin? A cross-site analysis of eddy flux tower measurements from the Brasil flux network, *Agric. For. Meteorol.*, *182-183*, 128–144, doi:10.1016/j.agrformet.2013.04.031.

Roberntz, P. (2001), Atmospheric carbon dioxide concentration, nitrogen availability, temperature and the photosynthetic capacity of current-year Norway spruce shoots, *Tree Physiol.*, *21*(12–13), 931–940, doi:10.1093/treephys/21.12-13.931.

Ruesch, A., and H. K. Gibbs (2008), *New IPCC Tier-1 Global Biomass Carbon Map For the Year 2000*, Oak Ridge National Laboratory, Oak Ridge, Tenn. [Available at the Carbon Dioxide Information Analysis Center, http://cdiac.ornl.gov.]

Saleska, S. R., et al. (2003), Carbon in amazon forests: Unexpected seasonal fluxes and disturbance-induced losses, *Science*, *302*(5650), 1554–1557, doi:10.1126/science.1091165.

Sanz, M., A. Carrara, C. Gimeno, A. Bucher, and R. López (2004), Effects of a dry and warm summer conditions on CO_2 and energy fluxes from three Mediterranean ecosystems, *Geophys. Res. Abstr.*, *6*, 03239.

Scharlemann, J. P., E. V. Tanner, R. Hiederer, and V. Kapos (2014), Global soil carbon: Understanding and managing the largest terrestrial carbon pool, *Carbon Manage.*, *5*(1), 81–91, doi:10.4155/cmt.13.77.

Schindler, D., M. Türk, and H. Mayer (2006), CO_2 fluxes of a Scots pine forest growing in the warm and dry southern upper Rhine plain, SW Germany, *Eur. J. For. Res.*, *125*, 201–212, doi:10.1007/s10342-005-0107-1.

Schmid, H. P., C. S. B. Grimmond, F. Cropley, B. Offerle, and H.-B. Su (2000), Measurements of CO_2 and energy fluxes over a mixed hardwood forest in the mid-western United States, *Agric. For. Meteorol.*, *103*(4), 357–374, doi:10.1016/S0168-1923(00)00140-4.

Sitch, S., et al. (2003), Evaluation of ecosystem dynamics, plant geography and terrestrial carbon cycling in the LPJ dynamic global vegetation model, *Global Change Biol.*, *9*(2), 161–185, doi:10.1046/j.1365-2486.2003.00569.x.

Smith, B., I. Prentice, and M. Sykes (2001), Representation of vegetation dynamics in the modelling of terrestrial ecosystems: Comparing two contrasting approaches within European climate space, *Global Ecol. Biogeogr.*, *10*(6), 621–637, doi:10.1046/j.1466-822X.2001.t01-1-00256.x.

Smith, B., W. Knorr, J.-L. Widlowski, B. Pinty, and N. Gobron (2008), Combining remote sensing data with process modelling to monitor boreal conifer forest carbon balances, *For. Ecol. Manage.*, *255*(12), 3985–3994, doi:10.1016/j.foreco.2008.03.056.

Smith, B., D. Wårlind, A. Arneth, T. Hickler, P. Leadley, J. Siltberg, and S. Zaehle (2014), Implications of incorporating N cycling and N limitations on primary production in an individual-based dynamic vegetation model, *Biogeosciences*, *11*(7), 2027–2054, doi:10.5194/bg-11-2027-2014.

Sokolov, A. P., D. W. Kicklighter, J. M. Melillo, B. S. Felzer, C. A. Schlosser, and T. W. Cronin (2008), Consequences of considering carbon-nitrogen interactions on the feedbacks between climate and the terrestrial carbon cycle, *J. Clim.*, *21*(15), 3776–3796, doi:10.1175/2008JCLI2038.1.

Staudt, K., and T. Foken (2007), *Documentation of Reference Data for the Experimental Areas of the Bayreuth Centre for Ecology and Environmental Research (BayCEER) at the Waldstein site*, vol. 35, pp. 1–35, Arbeitsergebnisse, Universität Bayreuth, Abt. Mikrometeorologie, Bayreuth, Germany.

Suni, T., et al. (2003), Air temperature triggers the recovery of evergreen boreal forest photosynthesis in spring, *Global Change Biol.*, *9*(10), 1410–1426, doi:10.1046/j.1365-2486.2003.00597.x.

Sutton, M. A., D. Simpson, P. E. Levy, R. I. Smith, S. Reis, M. Van Oijen, and W. De Vries (2008), Uncertainties in the relationship between atmospheric nitrogen deposition and forest carbon sequestration, *Global Change Biol.*, *14*(9), 2057–2063, doi:10.1111/j.1365-2486.2008.01636.x.

Tagesson, T., B. Smith, A. Löfgren, A. Rammig, L. Eklundh, and A. Lindroth (2009), Estimating net primary production of swedish forest landscapes by combining mechanistic modeling and remote sensing, *Ambio*, *38*(6), 316–324.

Takagi, K., et al. (2009), Change in CO_2 balance under a series of forestry activities in a cool-temperate mixed forest with dense undergrowth, *Global Change Biol.*, *15*(5), 1275–1288, doi:10.1111/j.1365-2486.2008.01795.x.

Thomas, R. Q., C. D. Canham, K. C. Weathers, and C. L. Goodale (2010), Increased tree carbon storage in response to nitrogen deposition in the US, *Nat. Geosci.*, *3*(1), 13–17.

Thomas, R. Q., G. B. Bonan, and C. L. Goodale (2013), Insights into mechanisms governing forest carbon response to nitrogen deposition: A model-data comparison using observed responses to nitrogen addition, *Biogeosci. Discuss.*, *10*(1), 1635–1683, doi:10.5194/bgd-10-1635-2013.

Thornton, P. E., J.-F. Lamarque, N. A. Rosenbloom, and N. M. Mahowald (2007), Influence of carbon-nitrogen cycle coupling on land model response to CO_2 fertilization and climate variability, *Global Biogeochem. Cycles*, *21*, GB4018, doi:10.1029/2006GB002868.

Thornton, P. E., S. C. Doney, K. Lindsay, J. K. Moore, N. Mahowald, J. T. Randerson, I. Fung, J.-F. Lamarque, J. J. Feddema, and Y.-H. Lee (2009), Carbon-nitrogen interactions regulate climate-carbon cycle feedbacks: Results from an atmosphere-ocean general circulation model, *Biogeosciences*, *6*(10), 2099–2120, doi:10.5194/bg-6-2099-2009.

Van Bodegom, P. M., J. C. Douma, J. P. M. Witte, J. C. Ordoñez, R. P. Bartholomeus, and R. Aerts (2012), Going beyond limitations of plant functional types when predicting global ecosystem-atmosphere fluxes: Exploring the merits of traits-based approaches, *Global Ecol. Biogeogr.*, *21*(6), 625–636, doi:10.1111/j.1466-8238.2011.00717.x.

van der Molen, M., et al. (2011), Drought and ecosystem carbon cycling, *Agric. For. Meteorol.*, *151*(7), 765–773, doi:10.1016/j.agrformet.2011.01.018.

Vesala, T., et al. (2005), Effect of thinning on surface fluxes in a boreal forest, *Global Biogeochem. Cycles*, *19*, GB2001, doi:10.1029/2004GB002316.

Vitousek, P., and R. Howarth (1991), Nitrogen limitation on land and in the sea: How can it occur?, *Biogeochemistry*, *13*(2), 87–115, doi:10.1007/BF00002772.

Vitousek, P. M., S. Porder, B. Z. Houlton, and O. A. Chadwick (2010), Terrestrial phosphorus limitation: Mechanisms, implications, and nitrogen-phosphorus interactions, *Ecol. Appl.*, *20*(1), 5–15.

von Randow, C., et al. (2004), Comparative measurements and seasonal variations in energy and carbon exchange over forest and pasture in South West Amazonia, *Theor. Appl. Climatol.*, *78*, 5–26, doi:10.1007/s00704-004-0041-z.

Wang, Y. P., R. M. Law, and B. Pak (2010), A global model of carbon, nitrogen and phosphorus cycles for the terrestrial biosphere, *Biogeosciences*, *7*(7), 2261–2282, doi:10.5194/bg-7-2261-2010.

Wårlind, D., B. Smith, T. Hickler, and A. Arneth (2014), Nitrogen feedbacks increase future terrestrial ecosystem carbon uptake in an individual-based dynamic vegetation model, *Biogeosciences*, *11*(21), 6131–6146, doi:10.5194/bg-11-6131-2014.

Wassen, M., H. Boer, K. Fleischer, K. Rebel, and S. Dekker (2013), Vegetation-mediated feedback in water, carbon, nitrogen and phosphorus cycles, *Landscape Ecol.*, *28*(4), 599–614, doi:10.1007/s10980-012-9843-z.

Williams, M., et al. (2009), Improving land surface models with FLUXNET data, *Biogeosciences*, *6*(7), 1341–1359.

Zaehle, S., and D. Dalmonech (2011), Carbon-nitrogen interactions on land at global scales: Current understanding in modelling climate biosphere feedbacks, *Curr. Opin. Environ. Sustainability*, *3*(5), 311–320, doi:10.1016/j.cosust.2011.08.008.

Zaehle, S., and A. D. Friend (2010), Carbon and nitrogen cycle dynamics in the O-CN land surface model: 1. Model description, site-scale evaluation, and sensitivity to parameter estimates, *Global Biogeochem. Cycles*, *24*, GB1005, doi:10.1029/2009GB003521.

Zaehle, S., S. Sitch, B. Smith, and F. Hatterman (2005), Effects of parameter uncertainties on the modeling of terrestrial biosphere dynamics, *Global Biogeochem. Cycles*, *19*, GB3020, doi:10.1029/2004GB002395.

Zaehle, S., A. D. Friend, P. Friedlingstein, F. Dentener, P. Peylin, and M. Schulz (2010), Carbon and nitrogen cycle dynamics in the O-CN land surface model: 2. Role of the nitrogen cycle in the historical terrestrial carbon balance, *Global Biogeochem. Cycles*, *24*, GB1006, doi:10.1029/2009GB003522.

Zaehle, S., P. Ciais, A. D. Friend, and V. Prieur (2011), Carbon benefits of anthropogenic reactive nitrogen offset by nitrous oxide emissions, *Nat. Geosci.*, *4*(9), 601–605, doi:10.1038/ngeo1207.

Zaehle, S., et al. (2014), Evaluation of 11 terrestrial carbon-nitrogen cycle models against observations from two temperate Free-Air CO_2 Enrichment studies, *New Phytol.*, *202*, 803–822, doi:10.1111/nph.12697.

Zenone, T. (2007), Measuring terrestrial CO_2 uptake in a short rotation forestry of poplar for bioenergy production: Comparison between biometric and micrometeorological techniques, PhD thesis, Univ. of Padova.

Zinke, P., A. Stangenberger, W. Post, W. Emanuel, and J. Olson (1984), Worldwide organic soil carbon and nitrogen data, ORNL/TM–8857, Tech. Rep., Oak Ridge National Laboratory, Oak Ridge, Tenn.